



**POLITECNICO
DI TORINO**

Master of Science in Mechanical Engineering

Master Thesis

Investigation through numerical simulation
of innovative gasoline powertrains
for a 48V Mild-Hybrid vehicle

Tutor

Prof. Federico Millo

Candidate

Lucia Colucci

Confidentiality agreement

This report contains some information which are not intended for publication. All the rights on the thesis, including the distribution through electronic media, are held by Politecnico di Torino. The content of this work cannot be published or transmitted to third parties without an explicit written authorization from Politecnico di Torino.

Clausola di riservatezza

Questo lavoro contiene informazioni non destinate alla pubblicazione. Tutti i diritti sul lavoro di tesi, inclusa la diffusione attraverso mezzi multimediali, sono detenuti dal Politecnico di Torino. Il contenuto di questo lavoro non può essere pubblicato o trasmesso a terzi senza un'approvazione esplicita e scritta da parte del Politecnico di Torino.

Abstract

The regulatory framework for light-duty vehicles concerning both greenhouse gasses and pollutants emissions is becoming increasingly demanding, leading car manufacturers to develop innovative technologies to comply with the limits imposed. Real Driving Emissions (RDE) regulations require the adoption of stoichiometric operation across the entire engine map also for downsized turbocharged gasoline engines, which usually take advantage of spark timing retard and mixture enrichment for knock mitigation. However, moving to a stoichiometric engine there is a severe deterioration of engine performance if no countermeasures are taken. In this context, the exploitation of Miller cycle and/or powertrain electrification is capable to improve engine and vehicle performance.

The aim of the work is therefore to evaluate, through numerical simulations, the potential of various electrified powertrain concepts equipped with a fully stoichiometric engine. In particular a P0 48V Mild-Hybrid Electric Vehicle (MHEV) architecture featuring an engine Millerization combined with an electric supercharger (eSupercharger) was analysed.

Firstly, a steady-state analysis of different engine concepts was performed aimed to evaluate the effects of various engine techniques, as the Millerization of engine cycle and/or the adoption of the eSupercharger. Secondly, a transient analysis was carried out evaluating different powertrain configurations equipped with the developed engine concepts. Vehicle performance were evaluated both in terms of elasticity manoeuvres and of CO₂ emissions for type approval and RDE driving cycles.

In order to investigate the theoretical potential of the combined effect of Millerization and electric boosting, different control strategies for the electric boosting were analysed during transient operation with a focus on fuel consumption. In particular, the base Equivalent Consumption Minimization Strategy (ECMS) technique was updated so that the electric power of the eSupercharger was taken into account in the powersplit optimization.

Sommario

Il quadro normativo per i veicoli commerciali leggeri, relativo sia alle emissioni di gas serra che di sostanze inquinanti, sta diventando sempre più esigente portando i produttori di automobili a sviluppare tecnologie innovative per rispettare i limiti imposti. Le normative Real Drive Emissions (RDE) richiedono l'adozione di una combustione stechiometrica nell'intera mappa motore anche per i motori a benzina sovralimentati downsized che, generalmente, sfruttano il ritardo di accensione e l'arricchimento della miscela per ridurre la probabilità di detonazione. Tuttavia, se non vengono prese opportune contromisure, passando ad un motore stechiometrico si verifica un grave deterioramento delle prestazioni del motore. In questo contesto il ricorso al ciclo Miller e/o l'elettrificazione del powertrain è in grado di migliorare le prestazioni del motore e del veicolo.

Lo scopo del lavoro è quindi quello di valutare, attraverso simulazioni numeriche, il potenziale di diversi sistemi di propulsione elettrificati dotati di un motore stechiometrico. È stato analizzato, in particolare, un veicolo con architettura P0 Mild-Hybrid 48 Volt equipaggiato con un motore Millerizzato combinato all'adozione di un sistema di sovralimentazione elettrico (eSupercharger).

In primo luogo, è stata effettuata un'analisi in stazionario su diversi scenari di motori al fine di valutare gli effetti di diverse tecnologie come la Millerizzazione del ciclo motore e/o l'adozione dell'eSupercharger. In secondo luogo, è stata condotta un'analisi in transitorio valutando diverse configurazioni di powertrain equipaggiati con i motori sviluppati. Le prestazioni del veicolo sono state valutate sia in termini di manovre di elasticità che di emissioni di CO₂ su cicli guida omologativi e su cicli guida RDE.

Al fine di studiare il potenziale della Millerizzazione combinata alla sovralimentazione elettrica, sono state analizzate, durante il funzionamento in transitorio, diverse strategie di controllo dell'e-booster con attenzione sul consumo di combustibile. In particolare, è stata aggiornata la tecnica Equivalent Consumption Minimization Strategy (ECMS) in modo da tener conto nell'ottimizzazione del powersplit, della potenza elettrica richiesta dall'eSC.

Acronyms

Item	Description	Unit
AT	After Treatment	-
BMEP	Brake Mean Effective Pressure	bar
BSFC	Brake Specific Fuel Consumption	g/kWh
BSG	Belt Starter Generator	-
CAD	Crank Angle Degree	-
CFD	Computational Fluid-Dynamics	-
CR	Compression Ratio	-
ECMS	Equivalent Consumption Minimization Strategy	-
EIVC	Early Intake Valve Closure	-
EM	Electric Machine	-
EMS	Energy Management Strategy	-
eSC	eSupercharger	-
EV	Electric Vehicle	-
FMEP	Friction Mean Effective Pressure	bar
FRM	Fast Running Model	-
ICE	Internal Combustion Engine	-
IMEP	Indicated Mean Effective Pressure	bar
HEV	Hybrid Electric Vehicle	-
LIVC	Late Intake Valve Closure	CAD
LHV	Low Heating Value	J/kg
MFB50	50 % Mass Fraction Burned Angle	CAD
MFB10-90	10 % - 90% Mass Fraction Burned Angle	CAD
MHEV	Mild-Hybrid Electric Vehicle	-
NEDC	New European Driving Cycle	-
OEM	Original Equipment Manufacturer	-

OOL	Optimum Operating Line	-
PI	Performance Index	-
PMEP	Pumping Mean Effective Pressure	bar
RDE	Real Driving Emissions	-
SoC	State of Charge	%
TC	TurboCharger	-
VVA	Variable Valve Actuation	-
WG	Waste-Gate	-
WOT	Wide Open Throttle	-
WPTC	Worldwide Harmonized Light-Duty Test Cycle	-
WLTP	Worldwide Harmonized Light-Duty Test Procedure	-
ZEV	Zero Emission Vehicle	-

Contents

Abstract	vi
Sommario.....	viii
Acronyms	xii
1 Introduction.....	1
1.1 Regulatory Framework Overview	2
2 Hybrid Electric Vehicles	7
2.1 Classification	7
2.2 48V Mild-Hybrid Vehicles	10
2.2.1 Architecture overview	10
2.2.2 Electric Supercharger	13
2.3 Energy Management Strategies	14
2.3.1 Equivalent Consumption Minimization Strategy	15
3 Steady-State Analysis.....	21
3.1 Engine Modeling Approach	21
3.2 Conventional Engine Concept.....	22
3.3 Electrified Engine Concepts	24
3.4 Results	26
3.4.1 Full Load.....	26
3.4.2 Part Load	29
4 Backward Kinematic Analysis	35
4.1 Case Study.....	36
4.2 Results	37
5 Dynamic Approach.....	43
5.1 P0 48V MHEV Architecture	43
5.2 Vehicle Model	44
5.3 Hybrid Control Modeling.....	47
5.4 Electric Supercharger Control Strategy	50
5.4.1 Rule Based Control	50
5.4.2 EMS Integrated eSC Control	52
5.5 Case study	53
5.6 Results	55
5.6.1 Fuel Consumption Evaluation	55
5.6.2 Transient Maneuvers Analysis	58
6 Conclusions.....	63

64	
65	
65	
66	
Bibliography	66

1 Introduction

The increasing rate of pollution due to vehicles has forced down all major nations to set new limits in terms of both emission rate and fuel consumption rate, for the present as well as for the future. To meet these limit values, the automotive industry is continuously developing more efficient and more environmentally technologies such as improved aerodynamics, lightweight design, more efficient transmission, regenerative braking, low rolling resistance tires etc. But almost all the technologies have reached their performance limits and their further improvement results in very small changes [1].

In this context the electrification process, undoubtedly represents an effective solution to meet environmental, economic and energy-security goals, and considering a sufficiently long-time frame, it will lead to a broad diffusion of Zero Emission Vehicles (ZEVs) [2]. Electric Vehicles (EVs) run on electrically powered engines, do not emit any pollutant substance and they could rely on clean energy source.

Although the EV's holds many promises, there are also several barriers to their penetration into the mainstream market today. Some are technologic, such as the capabilities of current battery technologies that restrict driving range and increase purchase price compared with conventional vehicles; others are related to consumer behavior and attitudes; and still others are related to the need to develop a charging network to support the vehicles and to address the possible effects of the new charging network on the electric grid [3].

Even though the end goal is zero emission, the propulsion system scenario is evolving towards a pure electrification through a gradual process that involves the simultaneous use of fuel energy and electric energy for propulsion purpose. Figure 1.1 shows a comprehensive overview of the European vehicle market in the near future.

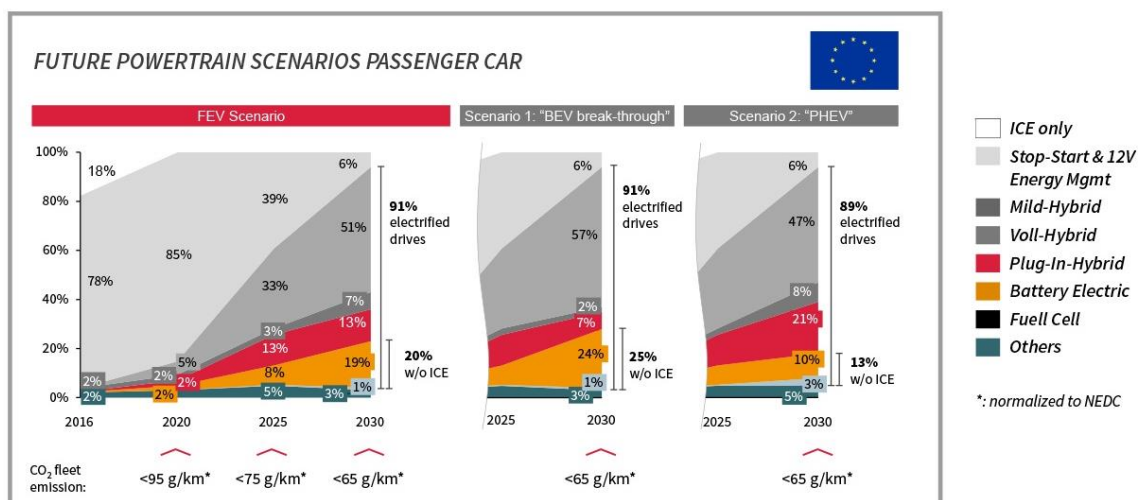


Figure 1.1 - Future Powertrain Scenarios Passenger Car in Europe [4]

1 Introduction

Hybrid Electric Vehicles (HEVs) represent the perfect bridge between the conventional powertrain equipped with the Internal Combustion Engine (ICE) and the pure electric vehicle. Hybrid electric vehicles are so defined because they combine two energy sources, complementing each other: a high-capacity storage (typically a chemical fuel) and a lower capacity rechargeable energy storage system that serves as an energy storage buffer and also as a means of recovering vehicle kinetic energy or to provide power assist [5]. They allow to exploit the benefits of gasoline engines and electric motors and can be configured to meet different objectives such as improved fuel economy, increased power, or additional auxiliary power for electronic devices and power tools.

In hybrid electric vehicles, the driver power demand is satisfied by summing together the ICE power and the Electric Machine (EM) power delivered. The possibility to manage in a flexible way the two energy sources permits to operate the engine more often in conditions where it is more efficient or less polluting. However, this flexible system leads in an increased complexity with respect to a conventional vehicle, requires a design challenge, specially related to chassis design and layout, multidisciplinary power management and optimization, system integration, and vehicle dynamics and control as well as an increase in the production price.

Currently due to their advantages, 48V mild hybrid systems are entering the mass market. Relatively simple integration into existing vehicle architectures and high efficiency of the components are the major advantages of 48V technology. The 48V electrification offers the possibility of adopting high power electrical auxiliaries that considerably increase the capabilities of a conventional vehicle. An example is the electric supercharger. Thanks to this electric device, the boost pressure can be supplied very quickly enhancing the engine transient behaviour during tip-in manoeuvres; it is able to fill the lack of response typical of a conventional turbocharger system due to its mechanical and fluid dynamic inertia (turbolag phenomenon).

1.1 Regulatory Framework Overview

The need to comply the pollutant emission target and the CO₂ regulation defines the “boundary conditions” in which the technological development of the powertrains for transport purpose can evolve. Every vehicle must be fully compliant with an approval procedure in order to be marketed.

The current legislation (Regulation 443/2009/EC, adopted on 23 April 2009) defines a limit value curve of permitted emissions of CO₂ for new vehicles according to the mass of the vehicle. The curve is set in such a way that a fleet average for all new cars of 130 grams of CO₂ per kilometer is achieved. From 2021, phased in from 2020, the EU fleet-wide average emission target for new cars will be 95 g CO₂/km ([6]). The official Test Procedure for homologation is the WLTP (Worldwide harmonised Light-duty vehicles Test Procedure), and the related driving cycle is the WLTC (Worldwide harmonised Light-duty vehicles Test Cycle). It substitutes the NEDC (New European Driving Cycle), used up to 2017.

Furthermore, the ongoing introduction of the Euro 6d-TEMP and RDE legislation will require both stricter limits and more rigorous assessment procedures: by September 2018,

1.1 Regulatory Framework Overview

the WLTP certification and the fulfilment of the Real Driving Emissions (RDE) limits including a PN reduction to $6 \cdot 10^{11}$ 1/km became mandatory for new registrations; the conformity factor (CF) for NO_x will be reduced up to 1 with Euro 6d regulations; moreover, a conformity check for CO will be introduced ([7]). Moreover, the avoidance of auxiliary emission strategies, such as mixture enrichment for component protection, will be mandatory for the compliance of the CO regulation.

According to the EU REGULATION (EC) 2017/1151 ([6]) for NOCV-HEV (Not Off-Vehicle Chargeable HEV) the values of CO₂ in terms of g/km can be compared if the charge sustaining condition is respected. The charge sustaining condition is satisfied if the term $C_{criterion}$ defined as the ratio between the depleted energy and the fuel chemical energy required for the driving cycle is lower than 0.5%:

$$C_{criterion} = \frac{E_{battery_depleted}}{E_{fuel}} < 0,005 \quad i. e. < 0,5\% \quad (1.1)$$

The legislation EC 333/2014 sets from the 2020 the long-term target as 95 grams of CO₂ per kilometer for the reference mass vehicle.

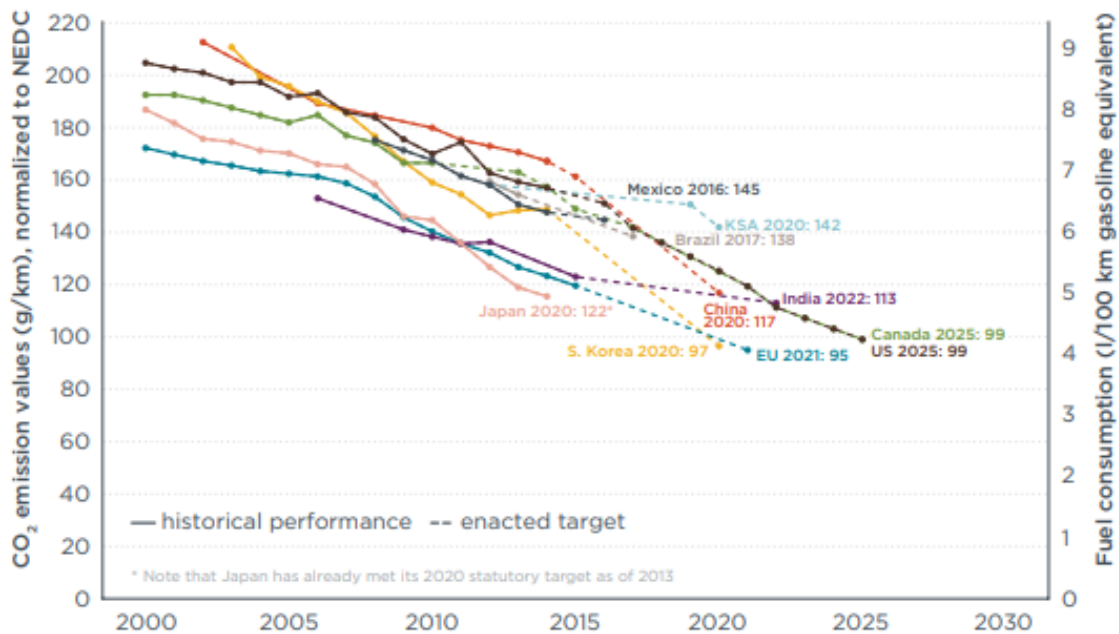


Figure 1.1 - Historical fleet CO₂ emissions performance and current standards (g CO₂/km normalized to NEDC) for passenger cars [9]

Regarding the Worldwide harmonised Light-duty vehicles Test Procedure, the measurement of light-duty vehicle emissions can be achieved by the chassis dynamometer which can simulate the driving on the real road. The procedure aims to closely reproduce the real driving activity in terms of vehicle velocity and acceleration. For this reason, the target speed profile is defined with a statistic approach; the WLTC is considered more representative of everyday driving with respect to the no longer used NEDC, and the homologation procedure closely reproduce the real driving condition (additional weight, electric loads etc.).

The new Real Driving Emissions test measures the pollutants emitted by cars while driven on the road. RDE procedure does not replace the WLTC laboratory test, but complements it and serves to confirm the WLTP results in real life, during real driving conditions. The

1 Introduction

driving conditions for the test include: low and high altitudes, year-round temperatures, additional vehicle payload, up and down-hill driving, urban roads, rural roads and motorways. Differently from a driving cycle, in which the engine operating points can be easily detected based on vehicle and engine data, during real driving condition the operating point cannot be defined a priori. The consequence is that the overall engine map should be optimized to compliance with the limits and this represents a major challenge for car manufacturers.

2 Hybrid Electric Vehicles

Hybrid electric vehicles combine an internal combustion engine with one or more electric machines for traction. The main advantage of HEVs is the possibility to split the total power request among the ICE and the EM, exploiting the optimum combination for fuel consumption minimization [10].

2.1 Classification

Several classification for the HEV's architecture have been proposed in literature, however one of the most widespread provides a classification based on the path followed by the power flow from the energy source to the wheels [11]:

- Series Hybrid Vehicles; only the electric machine provides power to the wheels. The EM receives electrical power from the battery or from a generator run by the ICE. In a series HEV the thermal engine is not connected to the wheels so it can operate in a high efficiency region while the fluctuating power required at the wheels is satisfied by the electric machine, taking advantages of its high efficiency in the overall operating map.

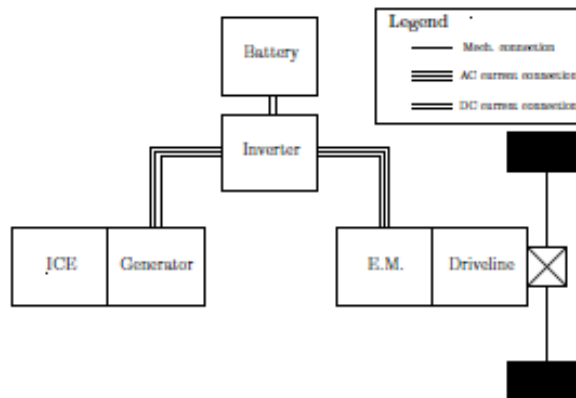


Figure 2.1 - Scheme of a Series Hybrid Configuration [10]

- Parallel Hybrid Vehicles: both the thermal engine and the electric machine simultaneously fulfil the driver power demand. The ICE and the EM are connected with a gear set, a chain, or a belt, so that their power is summed mechanically and then transmitted to the wheels. The control of such system is more complex compared to a series HEV, because it has a larger number of freedom degree for the power split operation.

2 Hybrid Electric Vehicles

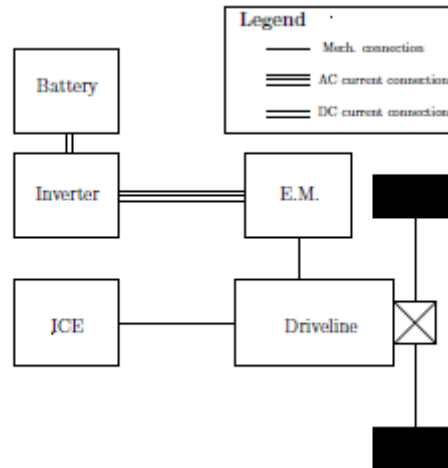


Figure 2.2 - Scheme of Parallel Hybrid Configuration [10]

- Complex Hybrid Vehicles: they combine the two design, series and parallel, by engagement/disengagement of one or two clutches. Complex HEVs combine in a very efficiency way the ICEs and EMs operations, unfortunately such systems have a high complexity of control strategy.

Another used classification regarding the hybrid electric vehicles is based on the position of the electric machine with respect to the other powertrain components. Based on this criterion it is possible to define five architectures: P0, P1, P2, P3 and P4. The powertrain configuration of the HEV system has an important impact on the performance and characteristics of the vehicle, in terms of integration cost, fuel efficiency and dynamic performance (powertrain torque enhancement), as shown in Figure 2.3.

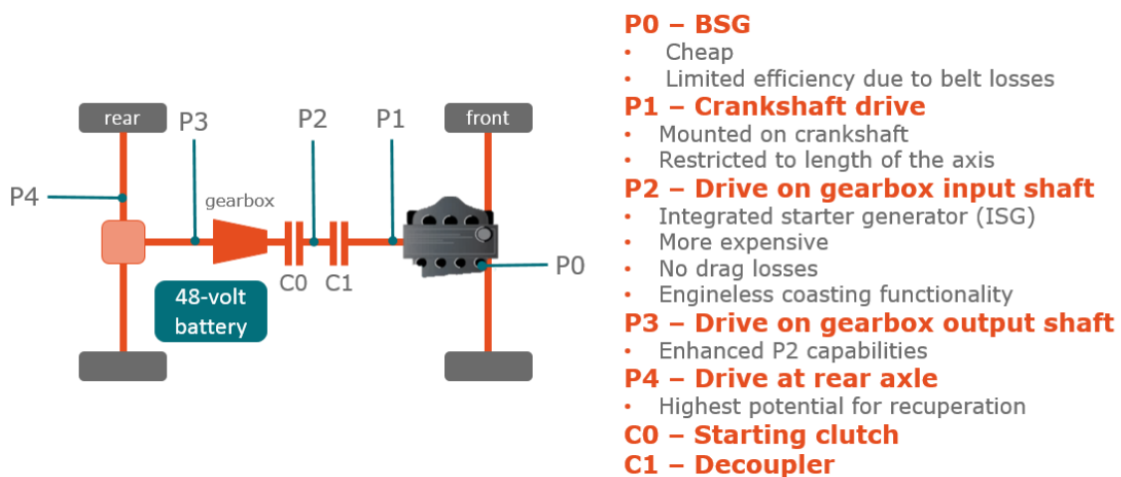


Figure 2.3 - MHEV powertrain architectures [12]

Lastly, the classification for HEVs formulated on the basis of the degree of hybridization or the power of the electrical system is reported in Table 2.1.

2.1 Classification

Parameter	Micro Hybrid	Mild Hybrid	Full Hybrid	Plug-in Hybrid
Battery voltage [V]	12	48 – 160	200 – 300	300 – 400
Electric machine power [kW] (motor)	2 ... 3	10 ... 15	30 ... 50	60 ... 100
Electric machine power [kW] (generator)	< 3	10 ... 12	30 ... 40	60 ... 80
EV mode range [km]	0	0	5 ... 10	< 50
CO ₂ estimated benefit [%]	5 ... 6	7 ... 12	15 ... 20	> 20

Table 2.1 - Synthesis of the types of hybrid HEV, in term of Battery Voltage, Electric Machine Power and potential fuel consumption benefit [13]

From Figure 2.4 it can be seen that as the electrical power available on board increases, the advantages in terms of fuel consumption and tank-to-wheel CO₂ emissions, as well as the cost of the product, also increased.

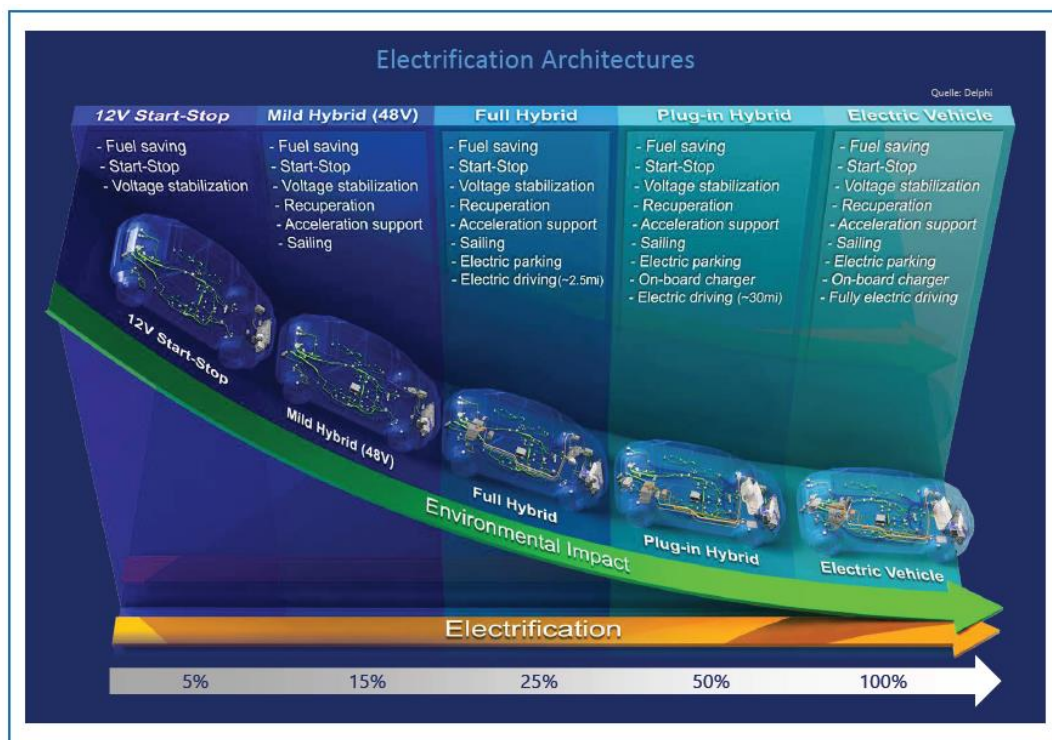


Figure 2.4 - Electrification architecture overview [14]

2.2 48V Mild-Hybrid Vehicles

The electrification of the powertrain system will play an important role in reducing the fuel consumption and engine-out emissions in the next few decades. Compared to the pure electric and full hybrid concept, the 48-Volt Mild Hybridization is the perfect bridge between the ageing 12V system and expensive high voltage electrification. It addresses regulatory requirements for emissions and safety and allows manufacturers to add cost effective features that consumers find desirable. As such, the 48V Mild Hybrid Electric Vehicles (MHEVs) are a good compromise that meet both regulatory, manufacturers and customer requirements.

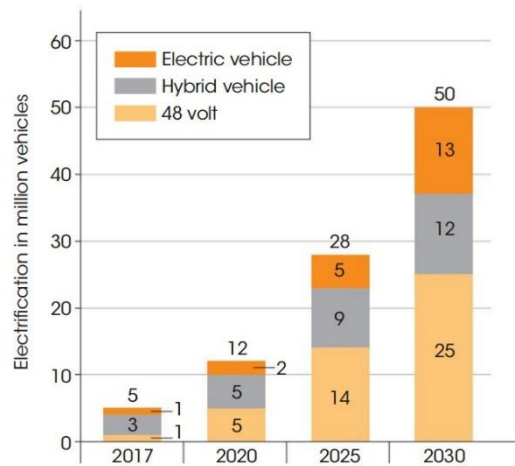


Figure 2.5 - Estimation of market penetration of hybrid electric vehicles by 2030
[Credit: Continental]

According to Continental, in the foreseeable future, there will be a continuous increase of market share for hybrid and pure electric vehicles. The biggest increase is expected to come from the 48V MHEV architectures, which will reach around 25 million units sold, until the year 2030 [15].

2.2.1 Architecture overview

In general, a 48V Mild-Hybrid system includes two voltage electric networks, respectively 12-volt and 48-volt connected together with a DC/DC converter. Currently the 48V electrical system does not replace the car's normal 12V electric network because that all the other low-cost accessories were designed to run on 12V and upgrading them to a higher voltage requires too large resources and support. The functionalities that the 48V-MHEV accomplish are:

- **Regenerative Braking:** a partial recovery of the kinetic energy of the vehicle during deceleration phases, that otherwise would be converted to unwanted and wasted heat by friction in the brakes. During this operation, the EM works as a generator and

stores the electrical energy in the battery: it is the most efficient method to charge the battery in a hybrid control strategy. How many energy can be recovered depends on the regenerative braking strategy adopted, on the size of the EM and on the hybrid architecture.

- Engine Load Shift: shift of the engine operating point towards the Optimum Operating Line (OOL) of the engine. If the engine operates at low load in order to increase the efficiency of the engine, the electric machine is set in generator mode and charges the battery. To compensate for the additional electric load, the engine load is increased and the engine operating point moves to a higher efficiency region.

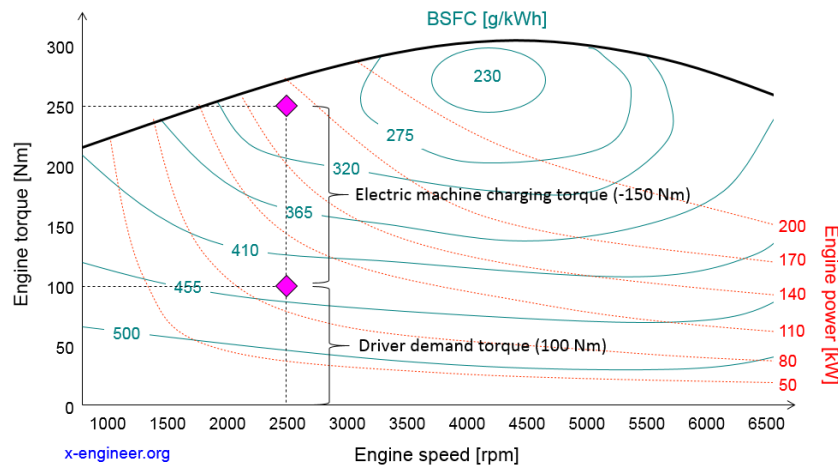


Figure 2.6 - BSFC improvement in HEV [12]

- Sailing or Coasting: these functionalities consists in disconnecting the engine from the transmission and stopping (or idling) the engine and filling the driver power demand only with the EM. In general, it is performed when the vehicle is travelling at a relative high speed and in low load engine condition that means poor engine efficiency.
- Electric Drive: possibility to keep the engine off during the starting phases and satisfy the overall driver power demand with the EM. In this way, the low engine load starting phases in which the ICE operates with low efficiency are avoided. Electric Drive function provides the maximum fuel economy benefit for P2, P3 or P4 MHEV architectures, since with a P0 architecture also pumping and friction power have to be taken in consideration, representing a surplus of power required for traction.
- Torque Fill and Torque boost: Torque fill means to compensate the driver torque demand which can not be delivered by the engine, with the electric machine torque. Especially in the low speed range, an ICE has a significant torque lag (delay). If the engine is operating in this region and the driver demands high torque, the difference between what the engine can deliver and what the driver demands can be compensated by the EM; the Torque boost means to boost (offset) the full load torque characteristic of an engine with the electric machine torque, improving the overall dynamic performance of the vehicle. On a MHEV, the total powertrain torque is the sum between the engine torque and electric machine torque.

2 Hybrid Electric Vehicles

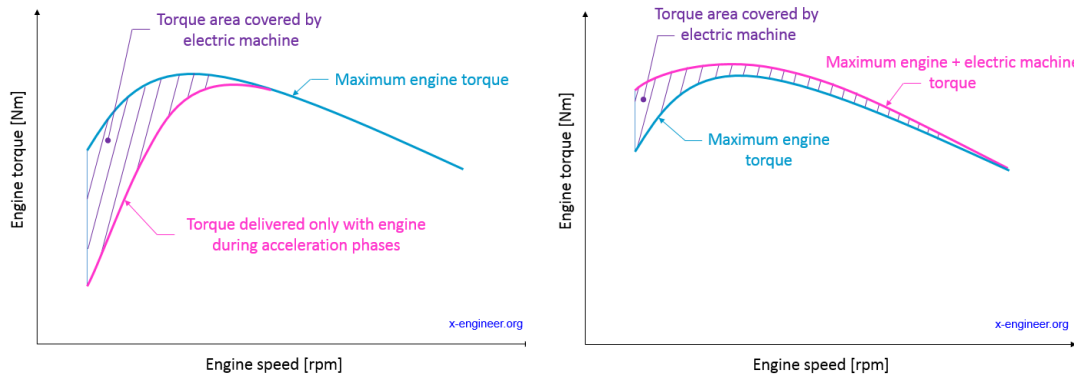


Figure 2.7 - Engine Torque Fill (left) and Torque Boost (right) with EM [12]

A Mild Hybrid Electric Vehicle architecture allows also to investigate a limited level of downsizing. The boost effect provided by the electric machine fills the eventual lack of peak power and torque; on the other hand, the engine operates on average at higher load and consequently in a higher efficiency region.

Another interesting potentiality for a dual voltage vehicle as a 48V MHEV is the possibility of using high power electrical auxiliaries (eCatalyst, eSupercharger, eWater Pump...). This can lead to an increase in fuel savings, due to the removal of additional loads of engine which can be directly operated by the high voltage of the 48V system, to after treatment warm-up, but also to improvements in drivability and comfort.

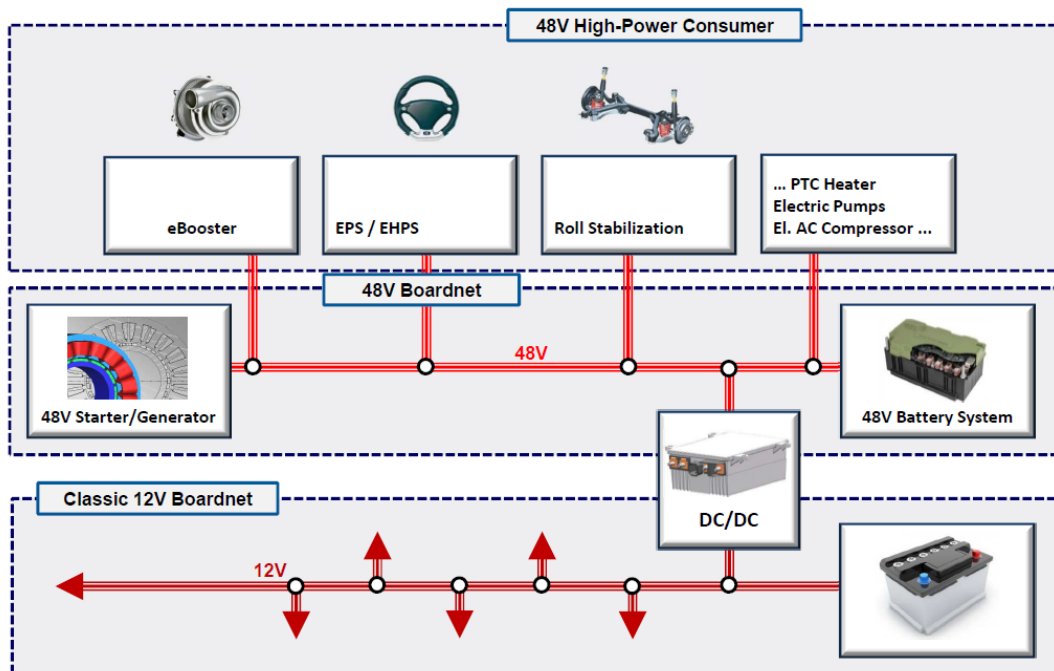


Figure 2.8 - Scheme of electric network for a 48V MHEV: dual voltage network and scheme of electrical ancillaries [16]

In the following section a detailed presentation of the electric supercharger will be reported.

2.2.2 Electric Supercharger

Electric supercharging is of interest for the engine operation under several aspects. For gasoline engine, the most significant potential is the opportunity to reduce fuel consumption and improve transient response, while for Diesel powertrains also to reduce engine emission during transient operation through a better Exhaust Gas Recirculation (EGR) control [17].

Electric Supercharger (eSC) also known as e-Booster or e-Compressor consists of a high-speed electric motor driving a compressor. The electric device has low inertia and low mechanical and electrical losses and the motor's response is instantaneous resulting in a fast transient response. It is designed to increase supercharging pressure and improve transient behaviour without increasing exhaust gases back pressure. The eSC supplements the engine in situations where the conventional turbocharger shows too long response times to reach the nominal working pressure (turbo lag phenomenon). Thanks to the electric compressor that intervenes instantaneously, even at low engine speeds, boost pressure can be supplied very quickly reducing the response delay of the motor to the driver actuation very to zero. Both upstream and downstream position of the eSC with respect to the turbocharger are possible: upstream layout is preferred for packaging requirements; downstream layout shows benefits for transient response.

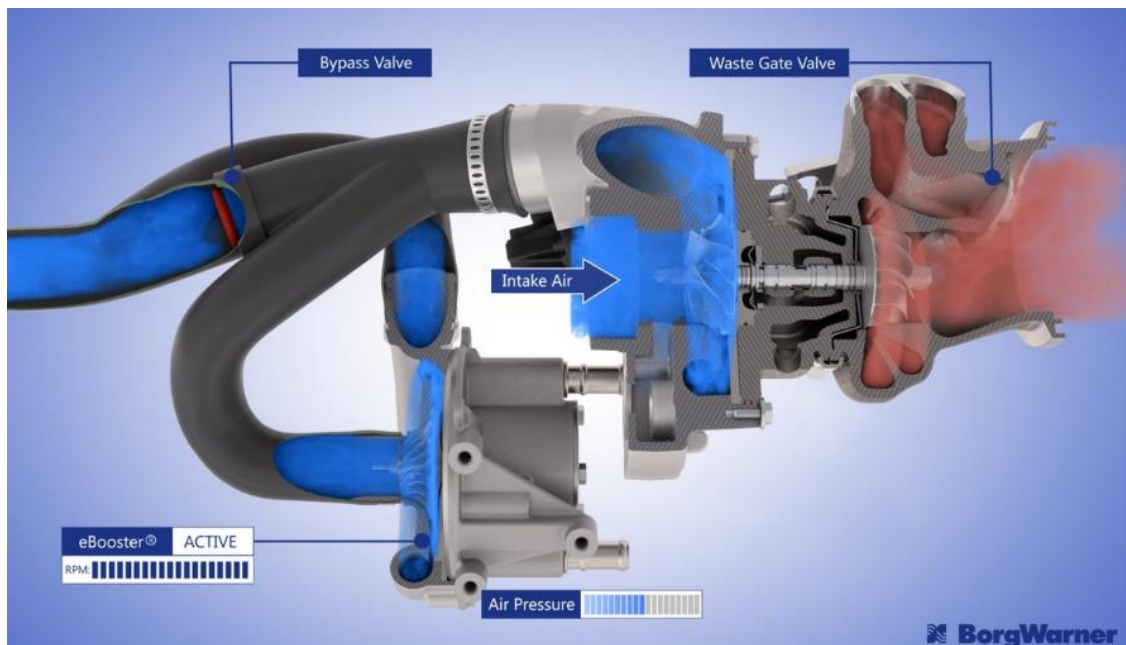


Figure 2.9 - Dual stage supercharging layout with eSupercharger [18]

This activity is aimed to assess not only transient performance benefits of the eSC, but also its potentialities for the fuel economy. It is worth to be highlighted that the introduction of this electric device introduces a higher level management complexity. Based on that, in the next section a general overview of the Hybrid Control Strategy will be presented, focusing on the research of a method capable to manage in an optimum way the overall electric energy consumption, aimed for propulsion purpose or not.

2.3 Energy Management Strategies

A conventional vehicle is propelled by only igniting fossil fuel in the internal combustion engine and converting the fuel energy into mechanical rotation and translation. The driver's desires are translated into actions by the low-level control (i.e the Engine Control Unit (ECU) determines the amount of fuel to be injected given the torque request). In contrast, HEV's are characterized by using several combination of a primary propulsion unit that can be fuel cell of an ICE or EM that can be an electrochemical storage system (i.e. battery) or an electrostatic super capacitor. Moreover, in addition to the mentioned components, at least one electric machine is necessary in any HEV to help propel the vehicle fully or partially [19]. The combination of electric and fossil fuel energy requires a high level controller called Energy Management Strategy (EMS) that defines how much power is delivered by each of the energy sources on-board of the vehicle through an optimal power-split. The choice on what to consider optimal depends on the specific application: usually the strategies tend to minimize the fuel consumption, but the optimization process could also include the minimization of pollutant emissions, the maximization of power delivery or in general a compromise among different goals [5]. As reported in [10], the EMS is divided into two control levels:

- Supervisory Controller: defines the optimum HEV functionality (e.g. pure electric drive, load point moving, regenerative braking...) taking into account all the state variables (driver power demand, state of charge of the battery, clutch status, vehicle speed...).
- Energy Management System: defines the optimal power-split between the energy sources on-board when the Supervisory Controller outputs a power split operation.

Figure 2.10 shows a schematic representation of how the EMS works.

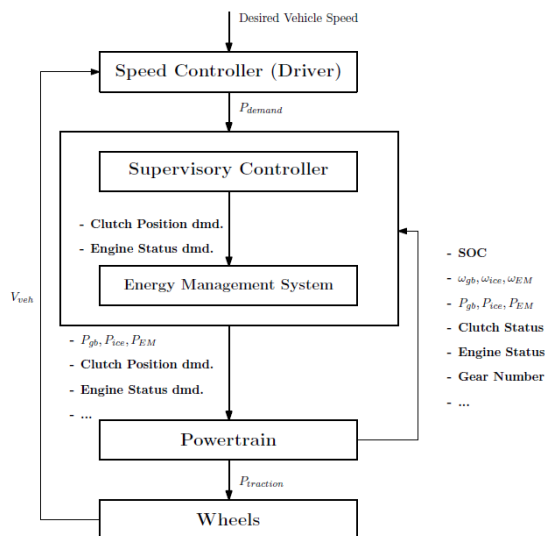


Figure 2.10 - The role of energy management system in a HEV [10]

According to [5] among the several families of hybrid control strategies proposed in literature, two general trends can be identified, namely *rule-based* and *model-based* optimization methods.

Rule Based energy management strategies rely on a set of rules to decide the output control to apply at each time. The rules applied are generally based on heuristics, intuition or on the result of an optimal global solution generated with more detailed mathematical models. Rule-based approaches are widely adopted for their feasibility and effectiveness in real-time implementation: they are characterized by low computational effort and do not require any a priori knowledge of the mission profile.

Model Based energy management strategies calculate the optimal output control by the minimization of a cost function over a fixed and known mission profile. These strategies cannot be used directly for real-time implementation due to their computational complexity and the knowledge required a priori of the driving cycle. Model-based approaches can be used for rules extraction for online implementation or as a benchmark solution to assess the performance of other control strategies. The model-based methods can be sub-divided into numerical and analytical approaches.

In numerical optimization methods, like dynamic programming [20], the entire mission profile is taken into account and the global optimum is found numerically.

Analytical optimization methods use an analytical problem formulation to find the solution in closed, analytical form or provide an analytical formulation that makes the numerical solution faster than the purely numerical methods. Among these methods, Pontryagin's minimum principle [21] is the most important. This category also include the Equivalent Consumption Minimization Strategy (ECMS) that it consists in the minimization at each time step of the optimization horizon, of an appropriately defined instantaneous cost function. This leads (ideally) to the minimization of the global cost function, if the instantaneous cost function (similar to an instantaneous equivalent fuel consumption) is suitably defined [5]. In recent years, several research projects have been conducted [22-23] focused on the development of an ECMS tool capable of being implemented on an online control unit, namely Adaptive ECMS. A more detailed explanation about the ECMS technique is reported in the following section.

2.3.1 Equivalent Consumption Minimization Strategy

The description about the ECMS reported here is taken from [5]. The ECMS is based on the concept that, in charge-sustaining hybrid electric vehicles, there will be a difference between the initial and final state of charge of the battery very small, at least negligible compared with the total energy used. This means that the battery is used only as an energy buffer: ultimately all energy comes from fuel, and the battery can be seen as an auxiliary, reversible fuel tank. Any stored electrical energy used during a battery discharge phase must be replenished at a later stage using fuel from the engine, or through regenerative braking. Two cases are possible at a given operating point:

1. The battery power is positive (discharge case) at the present time; this implies that at some future time the battery will need to be recharged, resulting in some additional fuel consumption in the future. How much fuel will be required to

2 Hybrid Electric Vehicles

replenish the battery to its desired energy state depends on two factors: (1) the operating condition of the engine at the time the battery is recharged; and (2) the amount of energy that can be recovered by regenerative braking. Both factors are in turn dependent on the vehicle load, and therefore on the driving cycle.

2. The battery power is negative (charge case): the stored electrical energy will be used to alleviate the engine load required to meet the vehicle road load, implying an instantaneous fuel saving. Again, the use of electrical energy as a substitute for fuel energy depends on the load imposed by the driving cycle.

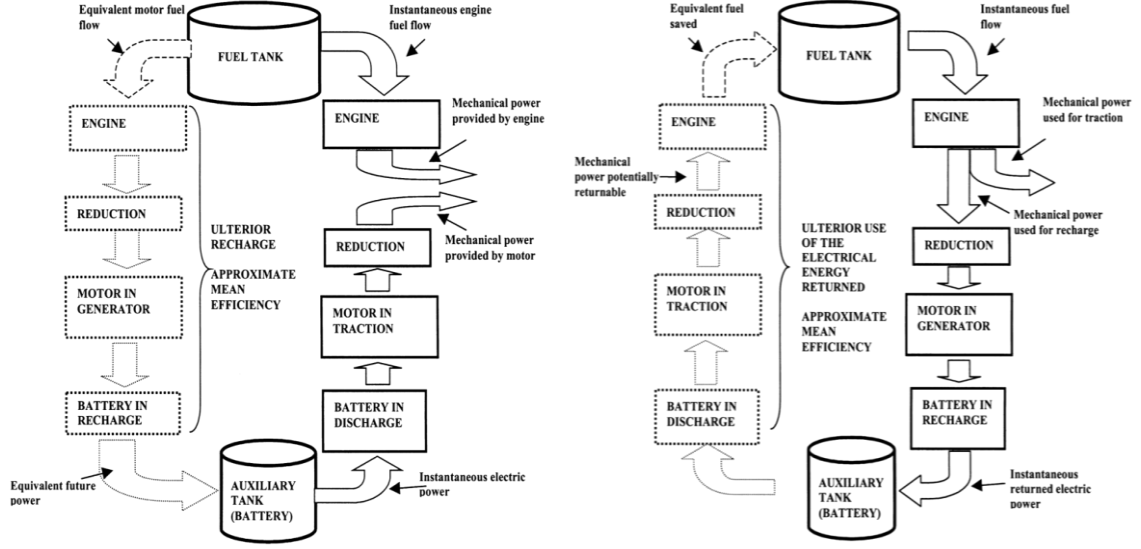


Figure 2.11 - Energy path during battery charge (right) and discharge (left) in a HEV [10]

The idea of the ECMS is to define an equivalent fuel consumption associated with the use of electrical energy. It corresponds to the future fuel flow required to recharge the battery or to the future fuel flow result from an increase of the State of Charge (SoC). The equivalent future fuel flow rate, $\dot{m}_{ress}(t)$ can be summed to the present real fuel mass flow rate $\dot{m}_f(t)$ to obtain the instantaneous equivalent fuel consumption $\dot{m}_{f,eq}(t)$:

$$\dot{m}_{f,eq}(t) = \dot{m}_f(t) + \dot{m}_{ress}(t) \quad (2.1)$$

The virtual fuel consumption $\dot{m}_{ress}(t)$ can be evaluated considering all the power losses in the flow between the engine and the battery in case of discharge (2.2) or charge (2.3) ([10]):

$$\dot{m}_{ress}(t) = \frac{1}{LHV} \frac{1}{\eta_{ICE} \eta_{batt,chg} \eta_{EM,chg} \eta_{trasm}} P_{batt}(t) \quad (2.2)$$

$$\dot{m}_{ress}(t) = \frac{1}{LHV} \frac{\eta_{batt,dis} \eta_{EM,dis} \eta_{trasm}}{\eta_{ice}} P_{batt}(t) \quad (2.3)$$

The chain of efficiencies through which fuel is transformed into electrical power and vice-versa represents the cost of the use of electricity; it is generally defined as equivalence factor it changes for each operating condition of the powertrain.

$$\dot{m}_{ress}(t) = \frac{s(t)}{LHV} P_{batt}(t) \quad (2.4)$$

2.3 Energy Management Strategies

The equivalence factor $s(t)$ is often set as a constant value, equal for charge and discharge case for the overall driving cycle: despite this simplification could have a great influence on the quality of the control strategy, it simplifies the complexity of the EMS. The selected value has to comply with charge-sustaining condition, and usually depends on the driving cycle itself, on the Driver Power Demand, on the strategy of regenerative braking [10].

As reported in [5], the following steps must be executed to implement ECMS:

1. Given the state of the system in terms of P_{req} , ω_{eng} , ω_{em} , SoC , . . . , identify the acceptable range of control $[P_{batt,min}(t) , . . . , P_{batt,max}(t)]$ which satisfies the instantaneous constraints (power, torque, current limits);
2. Discretize the interval $[P_{batt,min}(t) , . . . , P_{batt,max}(t)]$ into a finite number of control candidates;
3. Calculate the equivalent fuel consumption $\dot{m}_{f,eq}(t)$ corresponding to each control candidate;
4. Select the control value P_{batt} that minimizes $\dot{m}_{f,eq}(t)$.

3 Steady-State Analysis

3.1 Engine Modeling Approach

The engine operating maps used in this study were developed from GT-Power simulations. GT-Power is a vehicle and engine modeling software package, which uses nonlinear Navier-Stokes equations along with thermodynamic and phenomenological solvers to accurately predict engine behaviour [24].

The fluid-dynamics and thermal properties are function of 1 coordinate only, thus reducing the computational time with respect to a 3D CFD software with a level of accuracy good enough for the evaluation of engine performance.

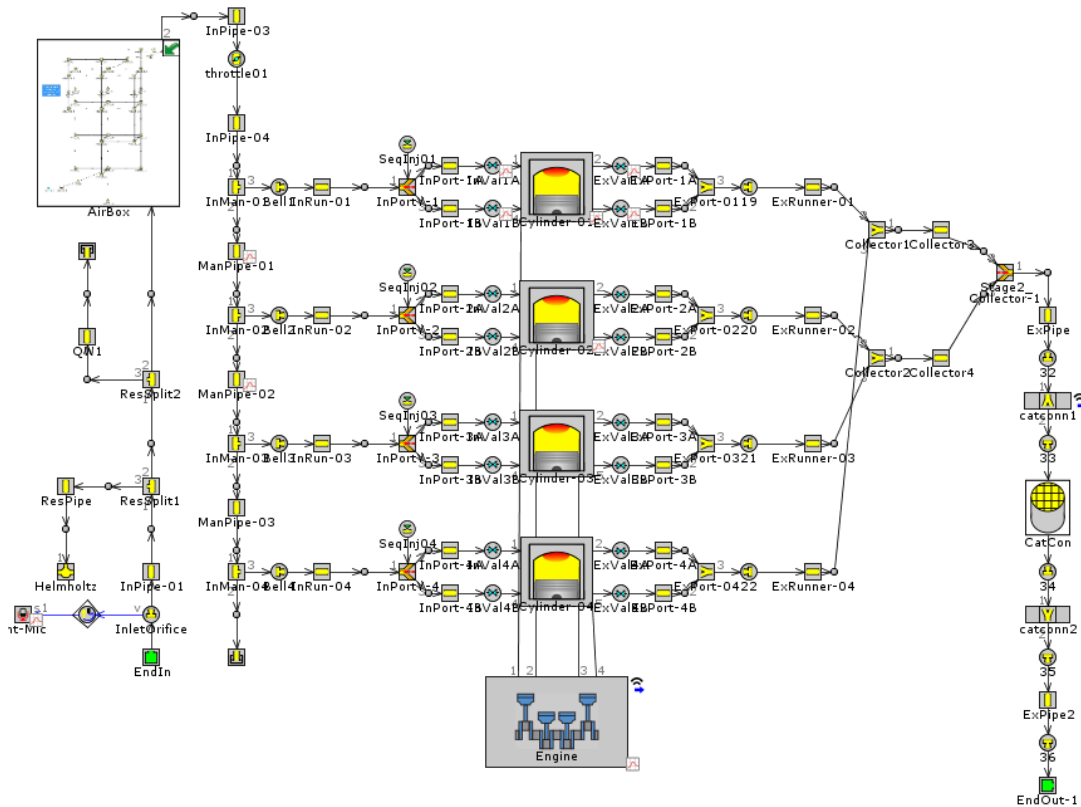


Figure 3.1 - GT-SUITE Engine Modelling example [25]

Although the 1D-CFD numerical simulation requires a relatively low calculation time, in order to have computational time adequate for long transients, as for example type approval and real driving emissions driving cycles, 1D model can be speed up at the expenses of the accuracy in the so-called Fast Running Model (FRM). As a reference the usual target for FRM engine model is 3 times the real time and below 5% difference in fuel consumption as well as

3 Steady-State Analysis

other engine parameters. This model was obtained through a process of reduction of the detailed model: reducing the number of flow volumes, lumping volumes together and increasing the time step size. Figure 3.2 shows an example of FRM assessment used for real time application.

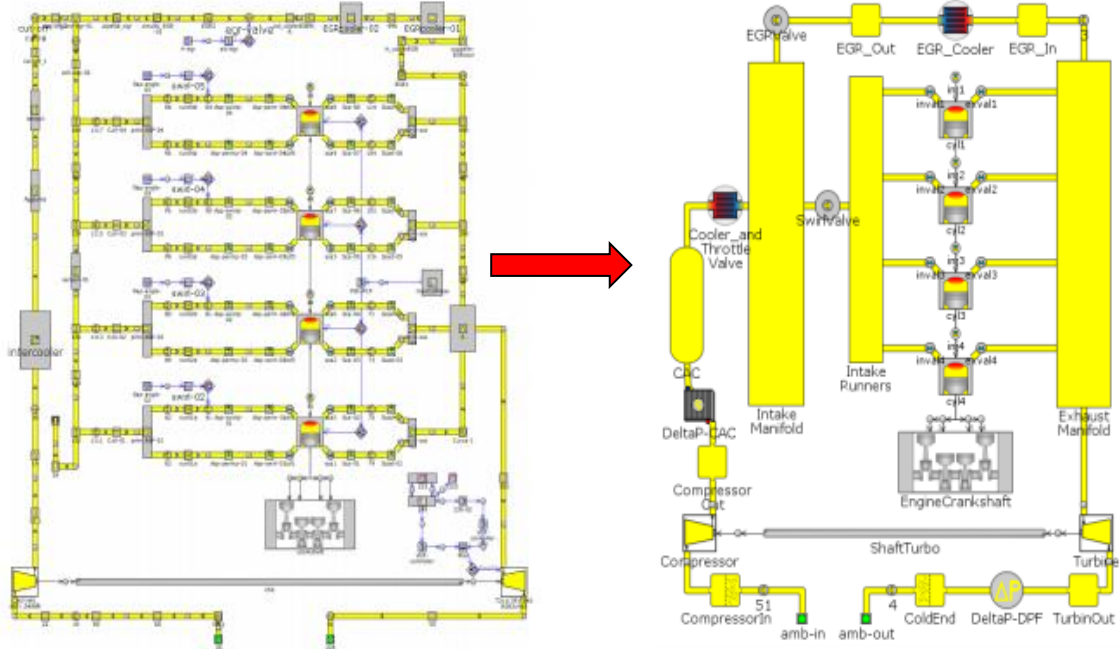


Figure 3.2 - Example of FRM assessment [26]

Fast running models do not allow to correctly simulate the high frequency dynamics effect such as wave propagation, but all the main fluid-dynamic phenomena are still well predicted, so they are suitable for purposes of this study.

Starting from the model developed in the study [27] on a stoichiometric turbocharged engine, various engine concepts have been developed to evaluate the effect of the Millerization of the engine cycle combined with the adoption of an electrical supercharger.

3.2 Conventional Engine Concept

The selected reference engine is the stoichiometric turbocharged gasoline engine that was developed and validated in [27]. The engine adopt a fully stoichiometric combustion in the overall map so it is fully Real Driving Emissions compliant. The main specifications of the engine are reported in Table 3.1.

3.2 Conventional Engine Concept

Parameter	Unit	Value
Displacement	cm ³	1368
Compression Ratio	-	9.8:1
Rated Power	kW	110 @ 5500 RPM
Rated Torque	Nm	243 @ 2750 RPM
Fuel Metering System	-	Port Fuel Injection
Air Management System	-	VVA

Table 3.1 - Engine Technical Data

In the engine model a certain number of controllers are implemented acting on Waste-Gate (WG) diameter of the turbocharging system and on throttle angle and taking into account all the hardware limitations as for example the compressor surge, knock tendency, maximum turbine inlet temperature and maximum TurboCharger (TC) speed.

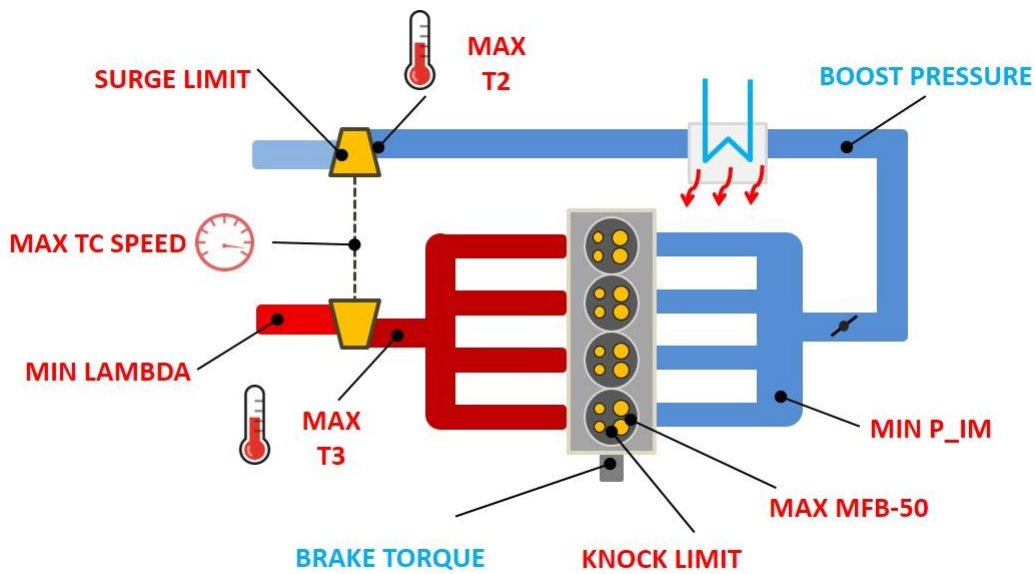


Figure 3.3 - Control-Based Model Engine Scheme [27]

On the intake manifold pressure engine map it is possible to define two regions corresponding to two different regulation types:

- Throttle regulation: the target brake torque can be achieved without turbocharging and regulating the throttle.
- Wastegate regulation: a turbocharging is needed and the engine will operate at Wide-Open Throttle (WOT) and regulating the wastegate in order to reach the boost pressure required for that operating points.

In Figure 3.4 these two regions are presented. The WOT curve, represented with the light blue point, is obtained maintaining the WG at the maximum equivalent diameter and imposing as target a very high values torque curve.

3 Steady-State Analysis

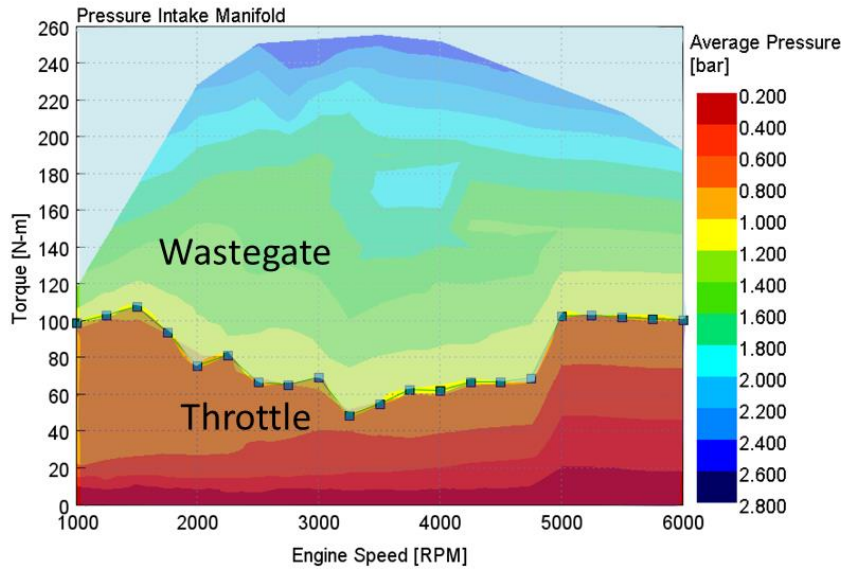


Figure 3.4 - Part Load Engine Control - Throttle and WG controlling regions [27]

In order to increase the full load brake torque curve and improve engine brake efficiency at high load region of the reference engine map, the conventional turbocharging system was coupled with an electric Supercharger and the Intake Valves Closure (IVC) was changed by adopting a *Millerization* of the engine cycle developing the engine concept presented as electrified engine concept.

3.3 Electrified Engine Concepts

The advantage of a Miller cycle for a turbocharged gasoline engine are explained in a detailed way in [28]: advancing (or delaying) the IVC the effective compression ratio decreases, leading to a lower charge temperature at the spark timing. If the supercharging is able to increase the amount of air in cylinder, the result will be a reduced likelihood of knock and a growth of engine performance. Because of the great effectiveness of this technique for knock mitigation, a Miller cycle is often coupled with the adoption of a larger compression ratio that improves engine brake efficiency at part load.

As reported in [27] the Compression Ratio (CR) was increased from the base value 9.8 to 12. In order to reduce the knock tendency, a Miller cycle was introduced in the high load engine map. The strategy used for Miller cycle actuation was Late Intake Valve Closure (LIVC) performed by keeping the valve at maximum lift for a certain crank angular interval and it was defined in order to maximize the brake torque at full load without exceeding the knock limit and the maximum T3 in the high load region. The LIVC for Miller cycle actuation can be performed with a Variable Valve Actuation (VVA) system, such as MultiAir technology. The combustion duration (10% to 90% Mass Fraction Burned angular duration) has been kept unchanged for the CR12 concepts.

Moreover, in order to satisfy the high level of boost pressure required in the Low and Torque (LET) region (up to 2750 RPM), a 48V electric supercharger was integrated, in upstream position with respect to the turbocharger.

3.3 Electrified Engine Concepts

The electric supercharger adopted for the study is a 48V eSupercharger (eSC). The main technical data are reported in the Table 3.2.

Parameter	Unit	Value
Compressor Max Speed	RPM	7500
Compressor Max Pressure Ratio	-	1.5
Compressor Max Corrected Mass Flow	kg/s	0.10
Compressor Peak Efficiency	-	0.82
Motor Nominal Torque	Nm	0.6 Nm
Motor Electrical Power	kW	5.3
Motor Peak Efficiency	-	0.85

Table 3.2 - Main technical specification of eSupercharger [27]

To evaluate the impact of eSupercharger, in GT-SUITE a flexible airpath layout has been modelled, allowing to switch from base layout (no eSC) to eSC upstream or downstream with respect to the turbocharger.

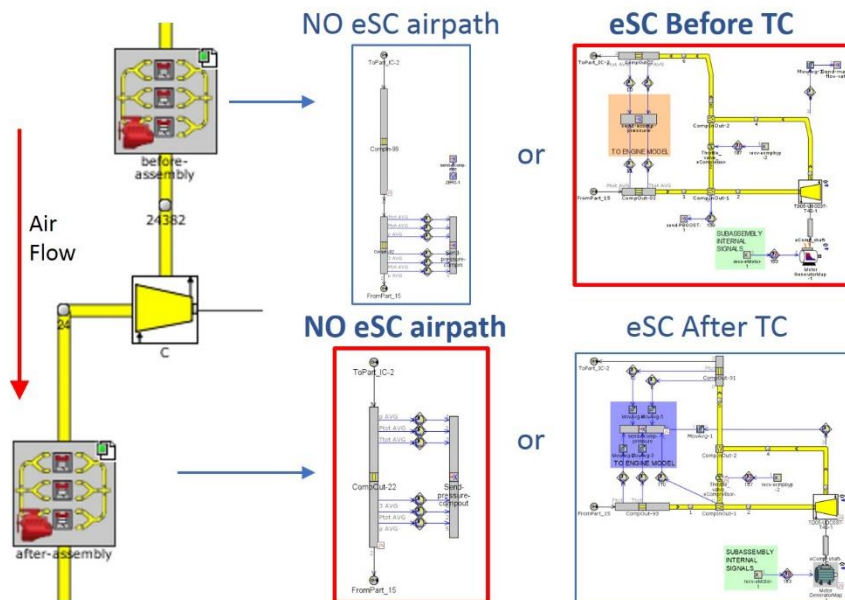


Figure 3.5 - Part Load Engine Control - Throttle and WG controlling regions [27]

With the adoption of eSupercharger it was necessary to update the controller used in the engine model. In the conventional engine model, without eSupercharger, at full load the wastegate was controlled in order to comply with knock, surge line and the other constraints, while in the electrified engine model boost pressure can be controlled both with WG and eSupercharger electric power. Supercharging the engine with the electric device does not involve any backpressure increase, as it happens closing the wastegate valve in a conventional TC system. Lower backpressure means lower residual fraction trapped in cylinder and consequently lower temperature at the start of compression, as well as lower pumping work. For these reasons at full load operation the electric supercharging rather than the turbocharging is preferred, and consequently the waste-gate is kept open if necessary. The influence of the Supercharger layout should be pointed out too: the eSC upstream of the TC is not able to charge larger amount of fresh air, it can be used only for

3 Steady-State Analysis

engine speed lower than 3000 RPM. At higher engine speed a by-pass valve will be opened, avoiding the eSupercharging operation [27].

3.4 Results

Several engine concepts were examined: the reference engine with a CR equal to 9.8 (Reference Engine), the high efficiency engine concept with a CR increased to 12 (Engine A), the Engine A featuring the adoption of the eSupercharger (Engine B) and finally the engine concept that features a CR equal to CR12, exploits a LIVC strategy for knock mitigation in the high load region and integrates the eSupercharger (Engine C).

In this section, the results in terms of steady-state performance are presented for the different engine concepts.

3.4.1 Full Load

In Figure 3.6, the brake torque and brake power at full load of the four engine concepts are reported.

Legend	CR	eSupercharger	Valve Strategy
Reference Engine	9.8	✗	MultiAir
Engine A	12	✗	MultiAir
Engine B	12	✓	MultiAir
Engine C	12	✓	MultiAir & Miller

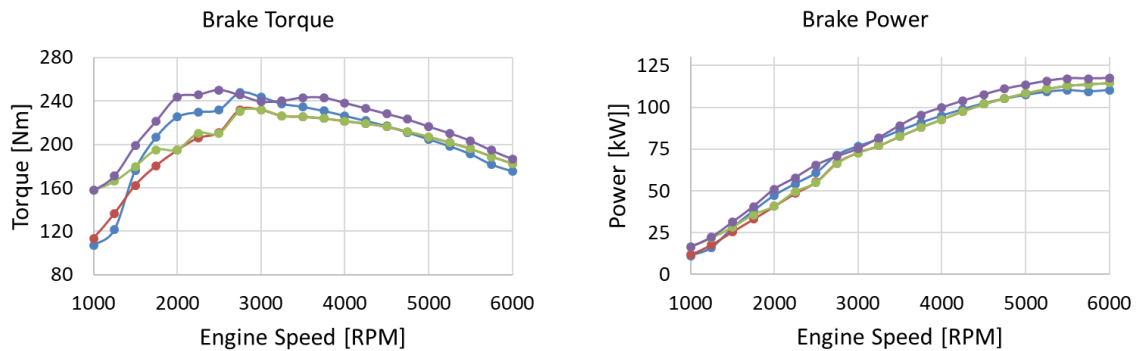


Figure 3.6 - Full Load Engine Concepts Results - 1

As far as the Engine A is concerned, the increment of the compression ratio from the base value 9.8 to 12, not combined with an actuation of the LIVC strategy, involves a deterioration of the engine performance in the low speed region since the tendency to knock at high load increases, so the MFB-50 must be delayed. The Engine A with respect to the Reference Engine shows a reduction of the maximum brake torque of about 14% at 2000 RPM; however the increment of brake efficiency deriving from the adoption of a CR equal to 12 produces a

slight increase of the maximum brake power in the high speed region (about 4% at 5750 RPM).

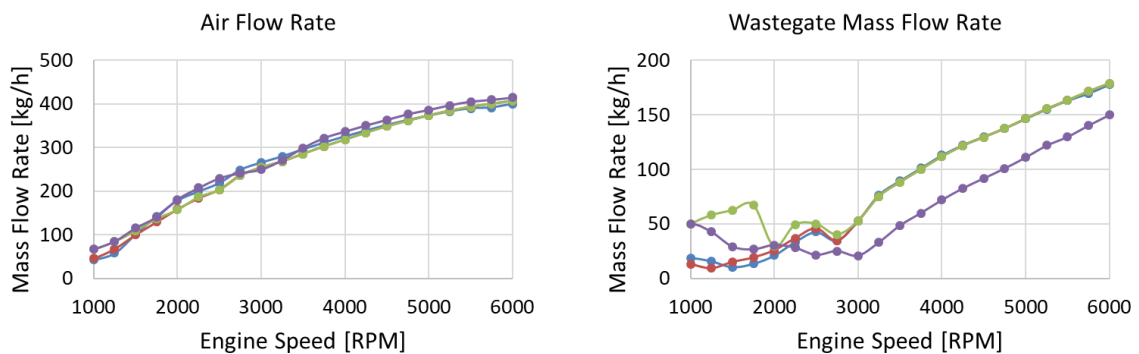
With regard to the Engine B, obtained through the adoption of an electric supercharger, an improvement in performance in the low speed region is obtained: the eSupercharger allows to increase the boost pressure by about 40% for engine speed less than 1250 RPM, however, beyond this speed there is the same deterioration of the brake torque curve found for Engine A.

Finally, the concept of Engine C is capable, by exploiting the advantage of the Miller cycle, of significantly increasing the maximum brake torque in the low speed region (more than 40% at 1250 RPM) and by about 5% in the high engine speed region. The increased boost level, required by the LIVC strategy, is obtained by exploiting the eSupercharger. In the low engine speed region, thanks to the two-stage supercharging, a maximum boost pressure up to 2.75 bar at 2000 RPM is available. Moreover, the Miller cycle reduces the knock likelihood: increasing the intake valve closure delay the charge temperature decreases and spark-advance can be increased enabling a significant improvement of the brake torque that reach a peak of 250 Nm at 2500 RPM. In addition, the LIVC strategy at high engine speed allows to enhance the maximum brake power reaching a peak of 117 kW at 5500 RPM. In this engine speed region, where the exhaust gases temperature is the main limitation, delaying the intake valve closure and consequently increasing the boost pressure, allows this temperature to be reduced.

	Ref. Engine	Engine A	Engine B	Engine C
Brake Torque [Nm]	243 @2750 RPM	232 @2750 RPM	232 @2750 RPM	250 @2500 RPM
Brake Power [kW]	110 @5500RPM	114 @6000 RPM	114 @6000 RPM	117 @5500 RPM

Table 3.3 – Performance Comparison for different Engine Concepts

Legend	CR	eSupercharger	Valve Strategy
Reference Engine	9.8	✗	MultiAir
Engine A	12	✗	MultiAir
Engine B	12	✓	MultiAir
Engine C	12	✓	MultiAir & Miller



3 Steady-State Analysis

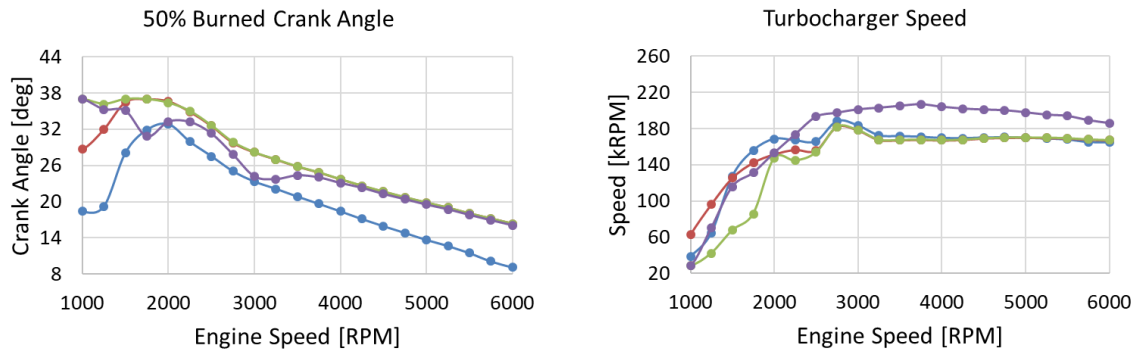
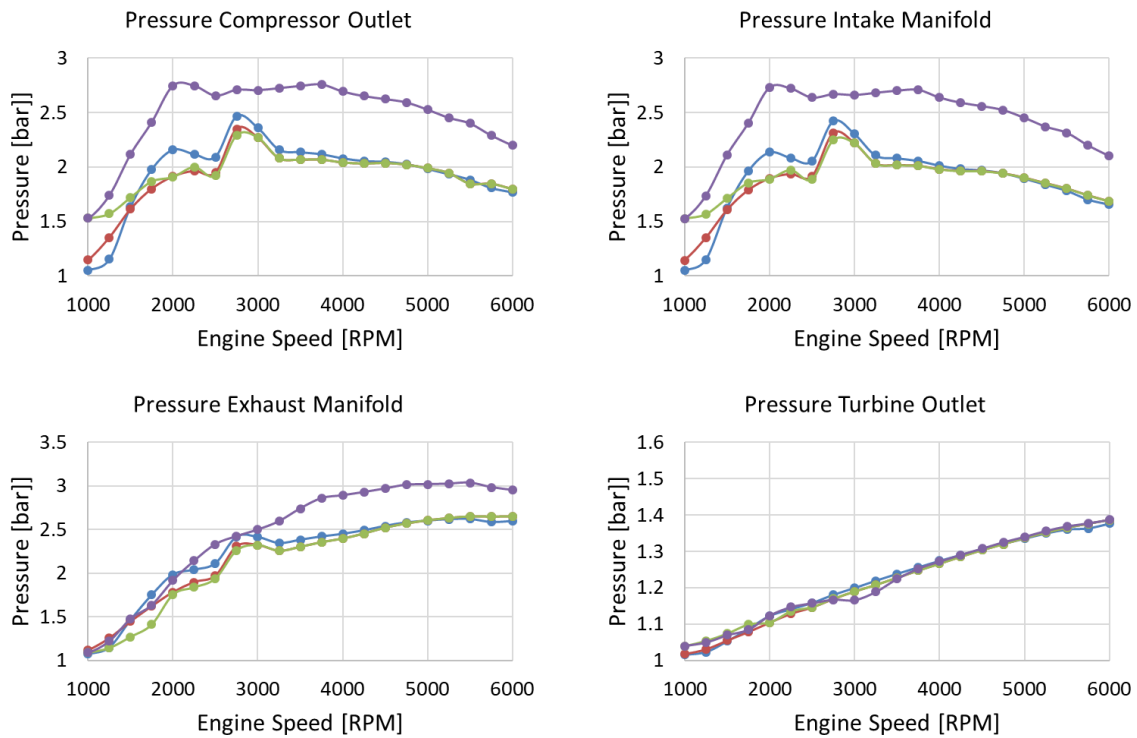


Figure 3.7 - Full Load Engine Concepts Results - 2

It is worth to be pointed out that with the Miller cycle, because of the increased boost pressure, the combustion must be delayed in order to keep unburned mass fraction at knock onset below 2%.

Legend	CR	eSupercharger	Valve Strategy
Reference Engine ■	9.8	✗	MultiAir
Engine A ■	12	✗	MultiAir
Engine B ■	12	✓	MultiAir
Engine C ■	12	✓	MultiAir & Miller



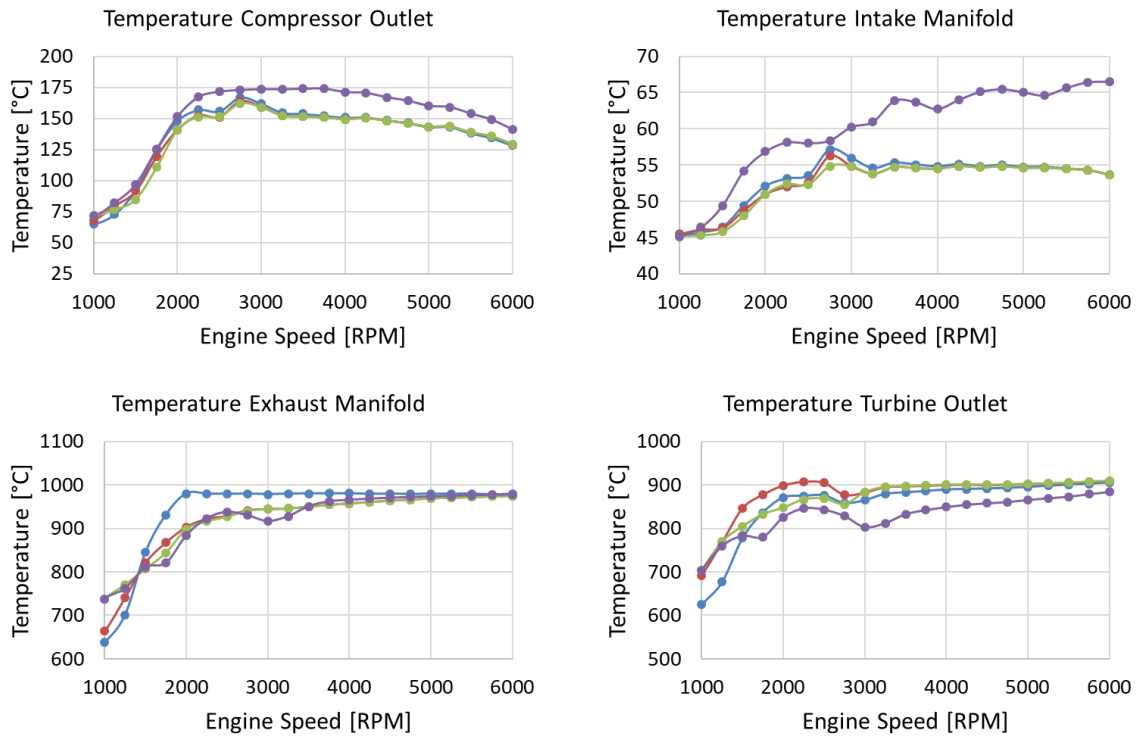


Figure 3.8 - Full Load Engine Concepts Results - 3

3.4.2 Part Load

Legend	CR	eSupercharger	Valve Strategy
Reference Engine	9.8	✗	MultiAir
Engine A	12	✗	MultiAir
Engine B	12	✓	MultiAir
Engine C	12	✓	MultiAir & Miller

The Figure 3.9 shows a comparison between the fuel flow rate maps of the developed engines compared to that of the Reference Engine.

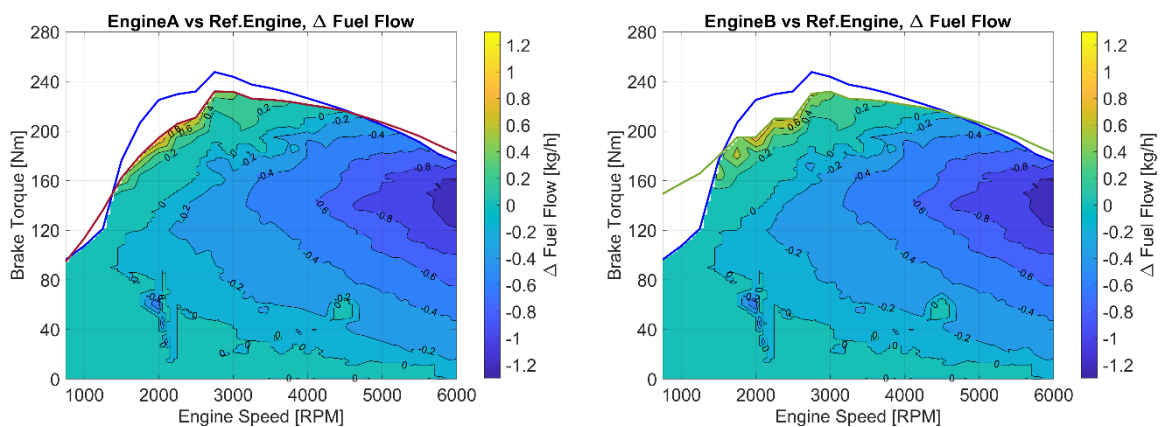


Figure 3.9 - Part Load Engine Concepts Comparison - 1

3 Steady-State Analysis

Both A and B Engines, thanks to the increase in efficiency resulting from the adoption of a higher compression ratio (increased to 12 from the base value of 9.8), allow fuel saving to be achieved on almost the entire engine map. In the low load engine region (up to 50 Nm) moving from low engine speed, where the differences in the fuel flow rate are negligible, toward higher engine speed the fuel saving increases to reach a benefit of about 3,7% at 5500 RPM. The most significant advantages are in the mid to high load region and high engine speed: for a brake torque between 100 and 160 Nm and an engine speed of over 3000 RPM there is a reduction in the fuel flow from 3% at 3000 RPM to 4.8% at 5500 RPM. For engine speed lower than 3000 RPM these benefits are attenuated because the increased knock tendency with the higher CR results in a delayed combustion phasing with a deterioration of the combustion efficiency, that at high load involves an increase in the amount of fuel required with respect to the Reference Engine: for brake torque values close to the full load curve and for engine speed between 1500 RPM and 2500 RPM, there is an increase in fuel flow rate up to 9% for the Engine A and up to 8% for the Engine B. The difference between the Engine A and Engine B in this region is due to the activation of the eSupercharger adopted in the Engine B: supercharging the engine with the electric device reduces the engine backpressure, with benefits in terms of pumping losses and knock mitigation. These engine concepts do not feature a Millerization of the engine cycle, therefore they are strongly limited by the constraints on the charge temperature at the end of the compression phase and the turbine inlet temperature.

Fuel Flow Rate Comparison				
Torque	1000 RPM	2000 RPM	3000 RPM	5500 RPM
40 Nm	- 0.5% Engine A	- 2% Engine A	- 2.7% Engine A	- 3.7% Engine A
	- 0.5% Engine B	- 2% Engine B	- 2.7% Engine B	- 3.7% Engine B
140 Nm	-	- 1.1% Engine A	- 3.3% Engine A	- 4.8% Engine A
	-	- 1.1% Engine B	- 3.3% Engine B	- 4.8% Engine B
190 Nm	-	+ 8.3% Engine A	0% Engine A	0% Engine A
	-	+ 7.5% Engine B	0% Engine B	0% Engine B

Table 3.4 - Fuel Flow Rate comparison for different operating points at part load with respect to the Reference Engine

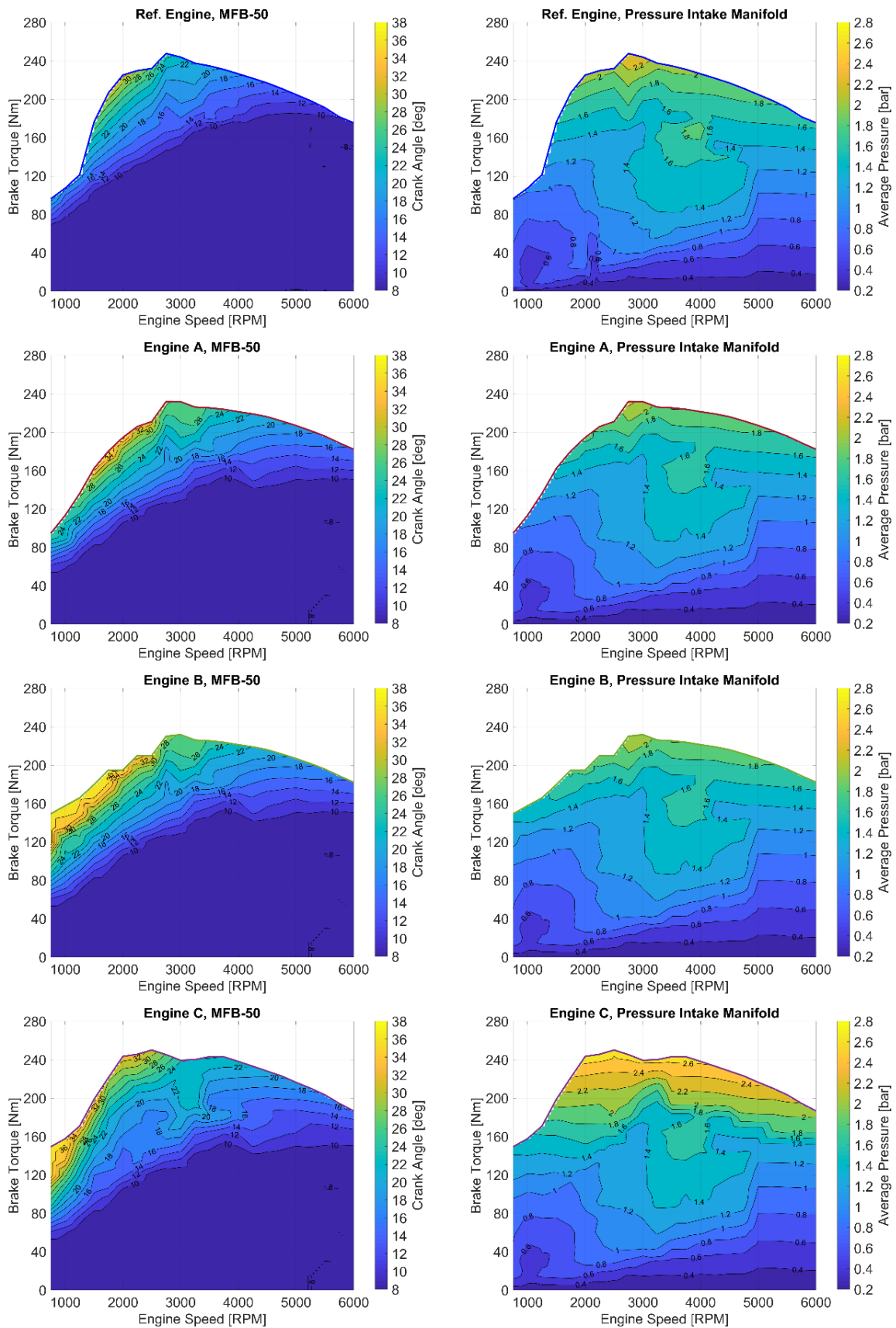


Figure 3.10 - Part Load Engine Concepts Results - 1

3 Steady-State Analysis

From Figure 3.10, which shows the comparison between the Engine C and the Reference Engine, it is possible to appreciate the effect of the Millerization of the cycle and the integration of the e-supercharger on fuel consumption. The Engine C is characterized by a globally higher efficiency with respect to the base configuration, which involves a reduction of the fuel flow rate over the entire engine map. Up to 1500 RPM and for low value of brake torque (up to 60 Nm) there is a negligible difference in fuel consumption, while at 3000 RPM the saving of fuel is in the order of 2.7% and at 5000 RPM it increases up to about 3.7% in the same load range. In the mid load region (up to 150 Nm), the fuel saving improves toward higher engine speed. At medium-high load (over 160Nm) and engine speed higher than 2500 RPM the fuel saving is reduced because the delayed combustion phase, necessary for the knock mitigation, has a detrimental impact on the combustion efficiency. In the high load region and for engine speed higher than 3000 RPM, the advantages related with the CR12 combined with the LIVC strategy are in the order of about 4%, while the advantages are of more than 9% in the range 1500-2500 RPM, where the electric supercharger reduces the engine backpressure, with benefits in terms of pumping losses and knock mitigation deriving from the decrease of the residual gas fraction.

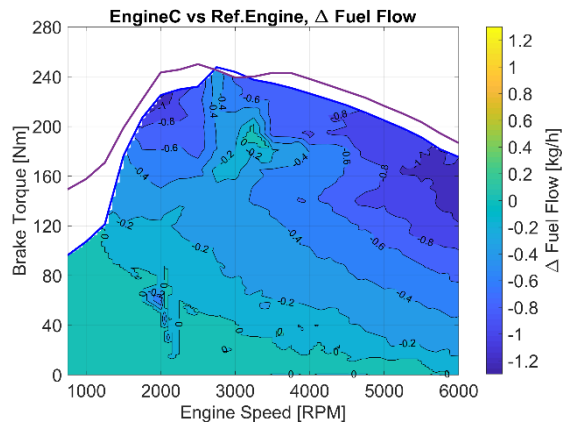


Figure 3.11 - Part Load Engine Concepts Comparison - 2

Fuel Flow Rate Comparison				
Brake Torque	1000 RPM	2000 RPM	3000 RPM	5500 RPM
40 Nm	- 0.5%	- 2%	- 2.7%	- 3.7%
140 Nm	-	- 4.5%	- 3.3%	- 4.8%
170 Nm	-	- 6%	-1%	-4.2%
190 Nm	-	- 7.8%	-2.5%	-

Table 3.5 - Fuel Flow Rate comparison for different operating points at part load with respect to the Reference Engine

Since it has been assumed that the combustion duration (MFB10-90) do not depend on the CR value and that therefore they have been kept unchanged for all engine concepts, the benefit of indicated efficiency could be underestimated for the engines featuring an increased compression ratio at part load operations.

4 Backward Kinematic Analysis

In order to evaluate the potential of the increase in the compression ratio and the adoption of Miller cycle for a stoichiometric turbocharged gasoline engine, a preliminary estimate was made, through a kinematic analysis, of fuel consumption over different driving cycles of a conventional vehicle equipped with the engine concepts investigated so far. The kinematic approach due to its low computational cost is the simplest way to predict vehicle's fuel consumption or emissions during a driving cycle. The approach is based on a backward methodology in which the vehicle speed and the road grade are supposed known and imposed on the vehicle.

Given the target speed profile and the gear shift profile, the engine speed can be determined from simple kinematic relationships starting from the wheel revolution speed and the total transmission ratio of the driveline, while, the engine torque (or the Brake Mean Effective Pressure, BMEP) is related to the traction force that should be provided to the wheels to drive the vehicle according to the chosen speed profile can be calculated from the main vehicle characteristics (i.e. vehicle mass, aerodynamic drag and rolling resistance) [10]. Once both engine torque and speed have been determined, it is possible to derive the instantaneous fuel consumption values by resorting to a 0D modeling, as shown in Figure 4.1. Finally, the cumulative quantities can be obtained by integrating the instantaneous ones over the driving cycle.

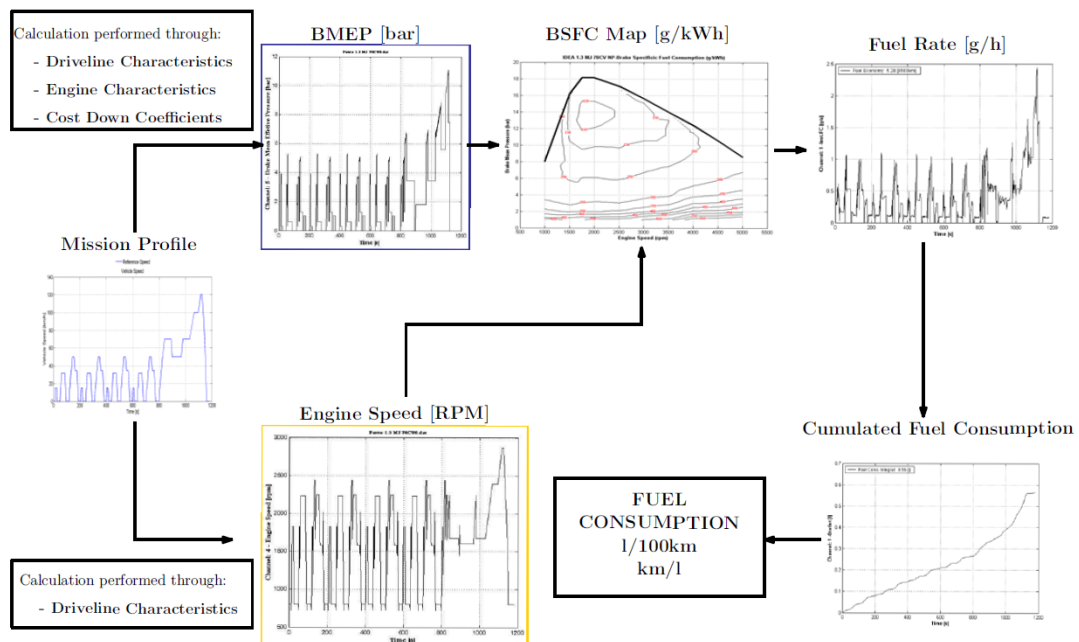


Figure 4.1 - Information flow in a backward model for fuel consumption calculation [10]

4 Backward Kinematic Analysis

It is worth to be pointed out that fuel consumption of the electrified engine concept (B and C Engines) is affected by the electric power required from the eSupercharger activation. Rather than referring to fuel consumption, the energy consumption over the cycle was taken into account, given by the sum of the fuel energy consumption and the energy required by the eSC. Starting from engine torque and speed it is possible to calculate the instantaneous electric power values requested by the eSC by resorting to the relative map obtained from the steady state analysis. Afterwards the electric energy can be obtained by the integration of the instantaneous values over the driving cycles. Finally, the electric energy is converted into a fuel energy consumption.

$$E_{tot} = E_{fuel} + \frac{E_{el,eSC}}{\eta_{el} \cdot \eta_{ICE}} \quad (4.1)$$

The assumption is that the engine working in a certain operating condition produces the power electric power required to the eSupercharger in order to reach a certain operating ICE condition. η_{el} is the overall electrical board net efficiency (alternator, battery charge and discharge), assumed constant and equal to 0.6 while η_{ICE} is the ICE efficiency, assumed constant and equal to 0.3.

The kinematic approach neglects all the dynamic phenomena considering transient conditions as a sequence of stationary states; therefore it is often used only for a first preliminary estimation of the fuel consumption or engine emissions of a motor vehicle, although the simulation results can differ significantly from the experimental data due to these simplifying assumptions. Moreover, the backward approach ensures that the driving profile will be exactly followed, but, on the other hand, there are no guarantees that a given vehicle will actually be able to meet the desired speed trace, since the power request is directly computed from the speed and it is not checked vs. actual powertrain capabilities [29]. Despite the introduced simplifications, the look-up tables approach is widely adopted, because it is simple to implement and requires a very low computational cost.

4.1 Case Study

Vehicle fuel consumption was evaluated for the investigated engine concepts on three driving cycles: the New European Driving Cycle (NEDC), the Worldwide Harmonized Light-Duty Test Cycle (WLTC) and a more dynamic RDE driving cycle, the RTS-95, whose characteristics are presented in Table 4.1. The target speed profile and the gear shift profile are the same for the different powertrain concepts. The gear shift is imposed on NEDC according to UNECE 83 [30] while on WLTC and RTS-95, according to [6], the gear shift pattern was computed by means of the Heinz Steven tool available in [31].

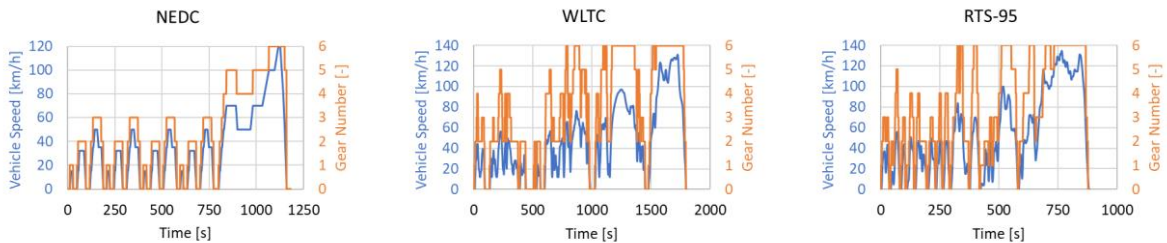


Figure 4.2 - Driving Cycles profiles

Parameter	Unit	NEDC	WLTC	RTS-95
Total time	s	1180	1800	886
Distance	km	11.03	23.27	12.93
Max. Velocity	km/h	120	131.3	134.45
Average Velocity	km/h	43.10	53.5	56.68
Max. Acceleration	m/s ²	1.04	1.58	2.62
Average Acceleration	m/s ²	0.51	0.41	0.73

Table 4.1 - Driving Cycles data [32]

The vehicle chosen as test case is a conventional compact SUV vehicle with the four engine concepts investigated and equipped with the same 6-speed manual transmission. The Table 4.2 shows the main features of the vehicle for the driving cycles selected.

Parameter	Unit	NEDC	WLTC	RTS-95
Vehicle Test Mass	kg	1470	1630	1630
Rolling Radius	m	0.333	0.333	0.333
Drag. Coeff. X Frontal Area	-	0.82	0.93	0.93

Table 4.2 - Vehicle Main Specifications for NEDC, WLTC and RTS_95

Gear	Transmission Ratio
I	4.154
II	2.188
III	1.486
IV	1.116
V	0.897
VI	0.767
Final Drive	4.118

Table 4.3 - Specifications of Manual Transmission

4.2 Results

In this section are presented the results obtained through the kinematic analysis in terms of reduction of CO₂ emissions and energy consumption achieved by the compact SUV vehicle selected as test case equipped with the different engine concepts investigated.

Legend	CR	eSupercharger	Valve Strategy
Reference Engine 	9.8	✗	MultiAir
Engine A 	12	✗	MultiAir
Engine B 	12	✓	MultiAir
Engine C 	12	✓	MultiAir & Miller

4 Backward Kinematic Analysis

The normalized CO₂ emission values are reported in Figure 4.3. It should be emphasized that in assessing the CO₂ emission only the engine fuel consumption was taken into account, not considering the energy expenditure required by the activation of the eSC for the supercharging operations requested at high loads.

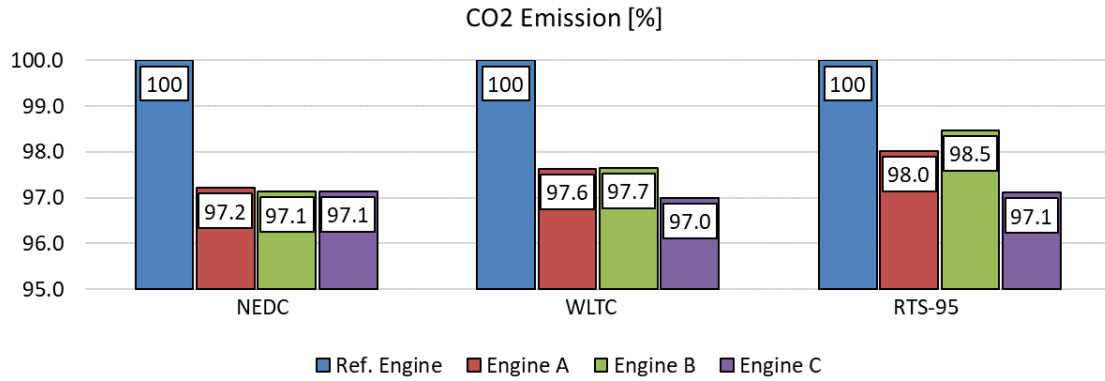


Figure 4.3 - Normalized CO₂ emissions for the NEDC, WLTC and RTS-95

As far as the NEDC is concerned, the same reduction of 2.9% is achieved in terms of CO₂ emissions for all engine concepts. Since the NEDC is not very aggressive, the engine operating points fall into the low-medium load region where the fuel consumption maps are only affected by the effect of the CR increase. The required BMEP levels do not require the activation of the eSupercharger nor of an actuation of the LIVC strategy.

The Engine C concept, which features a CR equal to 12, exploits a LIVC strategy for knock mitigation in the high load region and integrates the eSC, allows for a 3% reduction in CO₂ emissions even on the WLTC and the RTS-95. The engine C is the one that has a reduction in fuel flow rate on the entire engine map compared to that of the Reference Engine.

Both A and B Engines, which do not have a LIVC strategy, fail to obtain the advantages of the Engine C. The engine operating points on the WLTC and RTS cycles move towards the medium-high load region where the consumption maps present an increase in fuel flow rate due to the reduction in combustion efficiency due the adoption of increased spark timing retard necessary for knock mitigation.

In order to make a more realistic estimate of the benefits obtainable from the electrified engine concepts (B and C Engines), an energy analysis was carried out. The analysis was focused on the WLTC and RTS cycles as the power demanded to drive the vehicle according to the NEDC not require the activation of the eSC so the reduction of the fuel energy consumption is equal to the reduction of the CO₂ emissions.

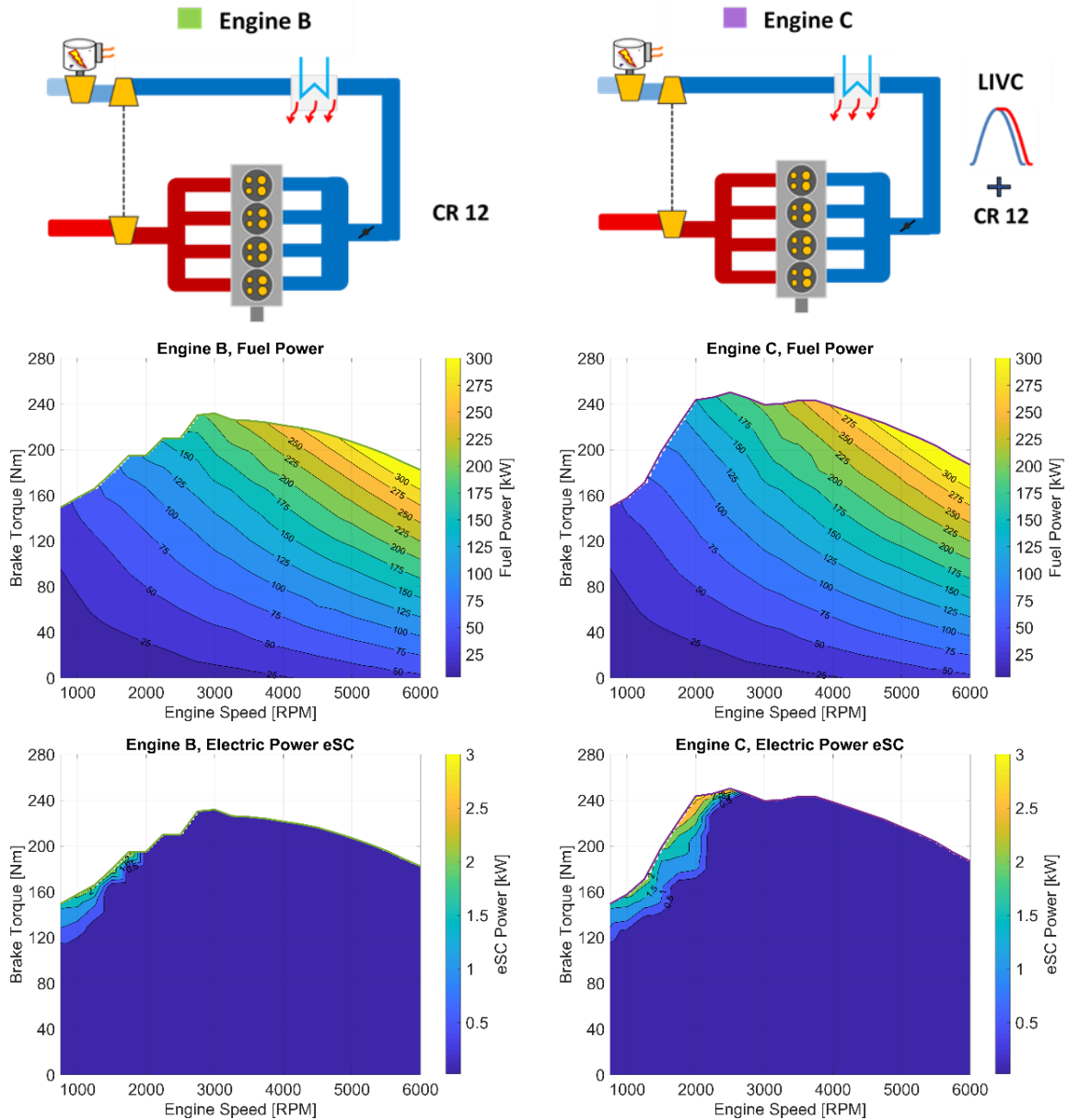


Figure 4.4 - Part Load Engine Concepts Results - 2

Figure 4.5 shows the percentage increase in energy consumption due to the eSC for the two electrified engines on the WLTC and RTS-95. Figure 4.6 shows the results in terms of energy consumption reduction. It can be noticed, the energy required to activate the eSC jeopardizes the reduction of fuel energy: the benefits are reduced to 2% and 0.8% for the engine B on WLTC and RTS-95 respectively, while to 2.6% and 1.8% for the Engine C.

4 Backward Kinematic Analysis

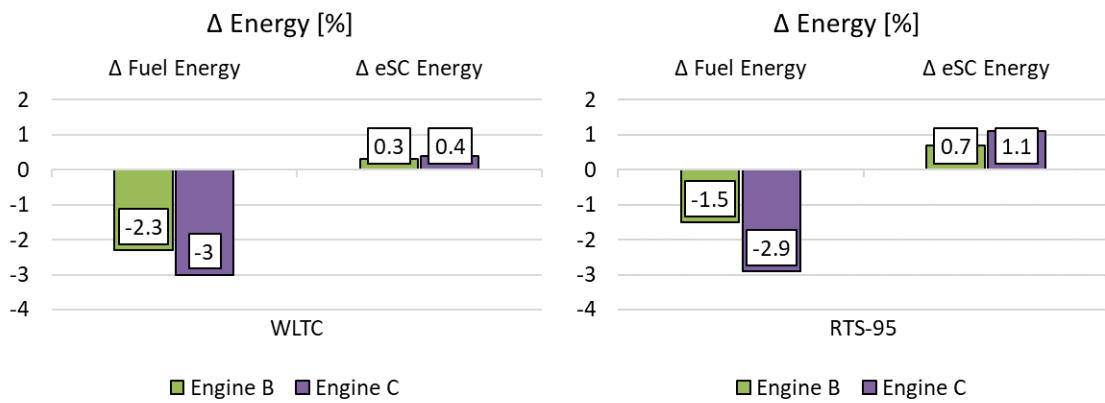


Figure 4.5 - Fuel Energy reduction and eSC Energy increase for the WLTC and RTS-95 with respect to the Reference Engine

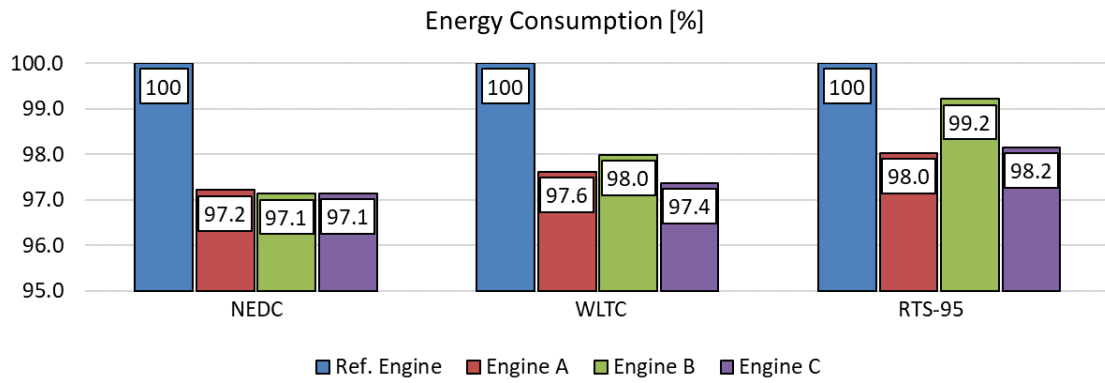


Figure 4.6 - Normalized Energy Consumption for the NEDC, WLTC and RTS-95

5 Dynamic Approach

In this chapter different powertrain concepts will be investigated by means of vehicle transient simulation. The study aimed to assess the potential of various electrified powertrain concepts equipped with a fully stoichiometric engine, evaluating in particular the potential of 48V electrification and the combined effect of Millerization and electric boosting. In addition, different control strategies for the electric supercharger were analysed during transient operation. The vehicle models were developed by using the software GT-SUITE and through a dynamic approach their performance were evaluated both in terms of CO₂ emissions on different driving cycles and of elasticity manoeuvres.

In the dynamic approach, it is possible to numerically solve both the response in longitudinal dynamics of the vehicle and the thermo-fluid dynamic behaviour of the internal combustion engine during transients. In the simulation, a driver model is introduced which, based on the actual speed of the vehicle, gives the powertrain control a specific power request to follow the speed target. The behaviour of the working fluid is estimated by numerical resolution of the system of equations of mass conservation, momentum and energy, in the hypothesis of one-dimensional flow, using a finite difference technique. Finally, usually for the modeling of the combustion process, appropriately calibrated 0D approximations are used, able to correctly reproduce the thermal release law when certain engine parameters change. This approach allows dynamic events, such as abrupt vehicle accelerations during tip-in manoeuvres, to be simulated with reasonable accuracy, but requires a higher computationally cost.

5.1 P0 48V MHEV Architecture

The hybrid architecture selected for the study is a P0 48V Mild-Hybrid Electric vehicle architecture because this mild hybrid topology combines a relatively low integration cost and considerable benefits in terms of CO₂ emissions reduction and dynamic performance boost. The 48V system has a limited impact on the existing vehicle architecture: the 48V electric machine is integrated into the already existing engine accessories belt drive, by replacing the 12V alternator (generator).

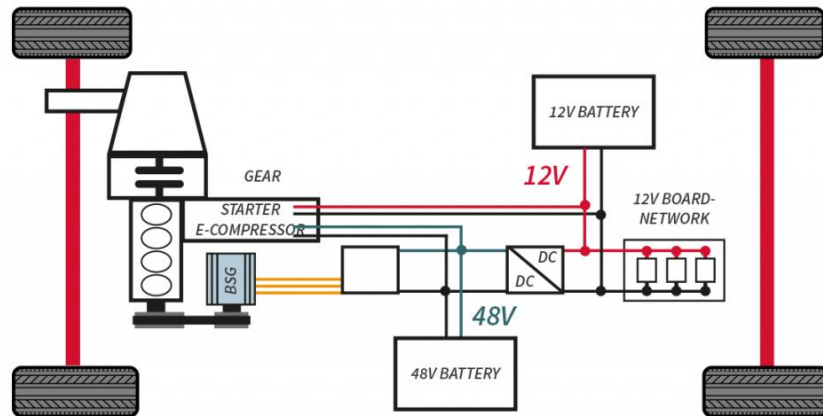


Figure 5.1 - Schematic representation of a P0 48V MHEV [33]

The Belt Starter Generator (BSG) provides electric propulsion to the vehicle in its function as a motor to increase the maximum power of the powertrain or to decrease the load of the ICE operating point as a result of the EMS optimization, while in its capacity as a generator it converts mechanical braking energy into electrical energy.

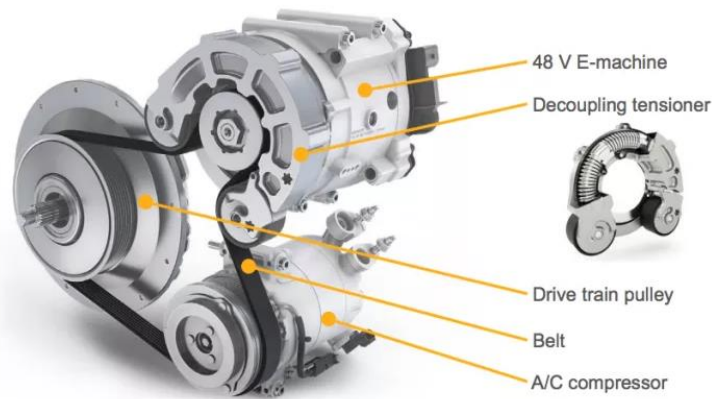


Figure 5.2 - 48 V Belt Starter Generator [34]

5.2 Vehicle Model

The vehicle model was developed using the GT-SUITE/Simulink coupled simulation. In GT-SUITE software was simulated the longitudinal dynamics analysis of the vehicle and the 1-D CFD analysis of the engine, while the implementation of supervisory control strategy and energy management system was carried through Matlab-Simulink routine. The vehicle model consists of five main parts: driver, driveline, engine, electric network and energy management strategy.

The driver is simulated by the “VehDriverAdvanced” block. This template is intended to be used as a vehicle driver who controls accelerator position, brake pedal position, transmission gear number and clutch pedal position. The model consists of a feed forward component which

calculates the engine load torque (or wheel braking torque) required for a targeted vehicle speed or acceleration. For this calculation, the 'VehDriverAdvanced' extracts key information from the drivetrain model. Once the reference load torque is calculated a standard Proportional-Integral (PI) controller is used to correct the demanded load from the engine or brakes to minimize the remaining error between target and instantaneous values [35].

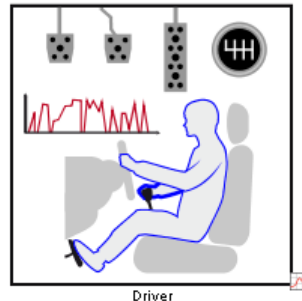


Figure 5.3 - GT-SUITE Driver Modeling

The driveline is composed by clutch, transmission, shaft, axles, brakes, tires and vehicle body. The several 1-D inertia components present are connected with either rigid/kinematic connections (single degree of freedom) or slipping/compliant connections (two degrees of freedom).

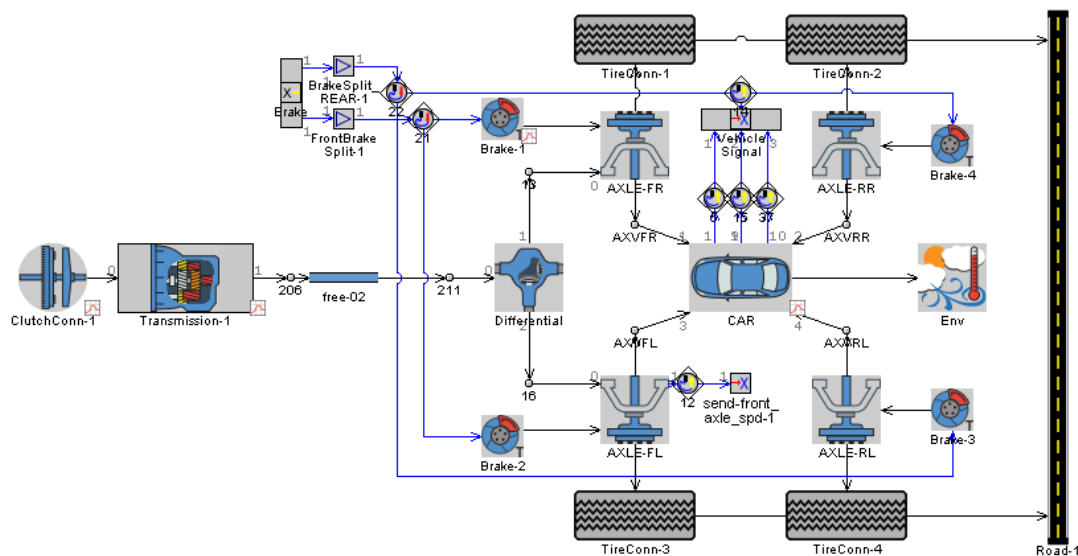


Figure 5.4 - GT-SUITE Vehicle Subsystem

Regarding the engine model, a 1D-CFD FRM was used. The engine is controlled by means of throttle and wastegate controllers. They translate an input of engine power demand into a boost pressure target and an intake manifold pressure target. Regarding the combustion, an imposed Wiebe profile was adopted, that is function of the MFB-50 and MFB 10-90. Those target values of pressures and combustion timing are obtained from the maps defined in steady-state simulation complying with the engine limitations (compressor surge, maximum turbocharger speed, knock tendency, maximum turbine inlet temperature).

Regarding the electric network, the main components are alternator, starter and batteries. The electric machines are modeled by the "MotorGeneratorMap" template using a map-based efficiency for the electro-mechanical conversion. Two electric networks in have been modeled

5 Dynamic Approach

in sub-assemblies that can be easily interchanged in order to reproduce a conventional 12 V electric network and a dual voltage 12+48 V electric network.

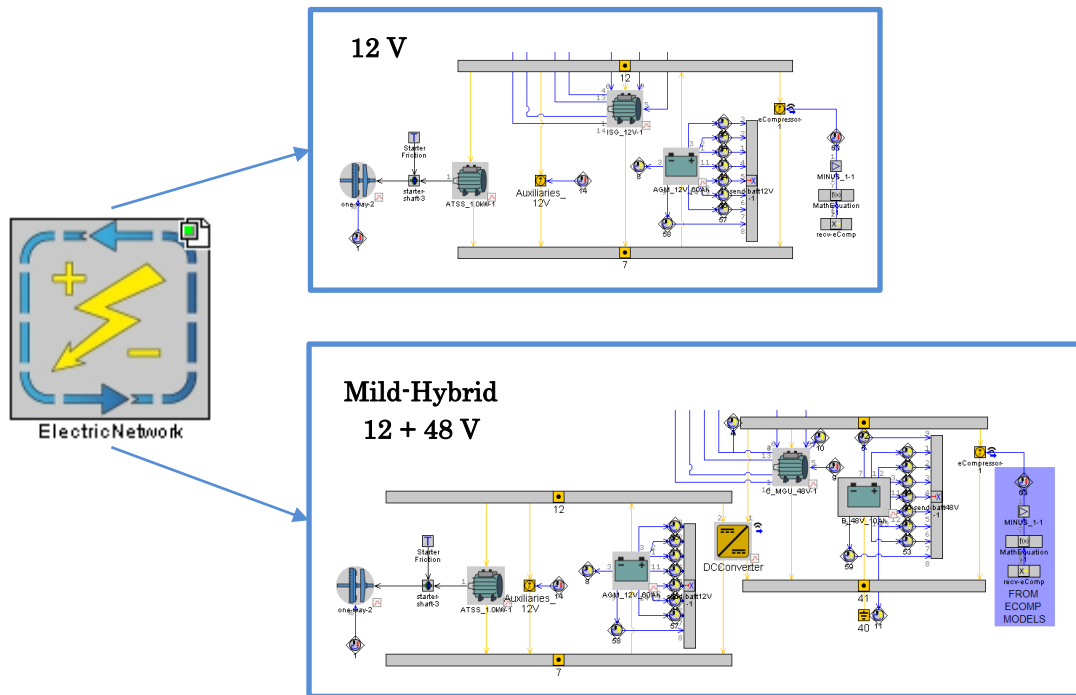


Figure 5.5 - GT-SUITE Electric Modeling; 12 V and 12+48 V sub-systems [27]

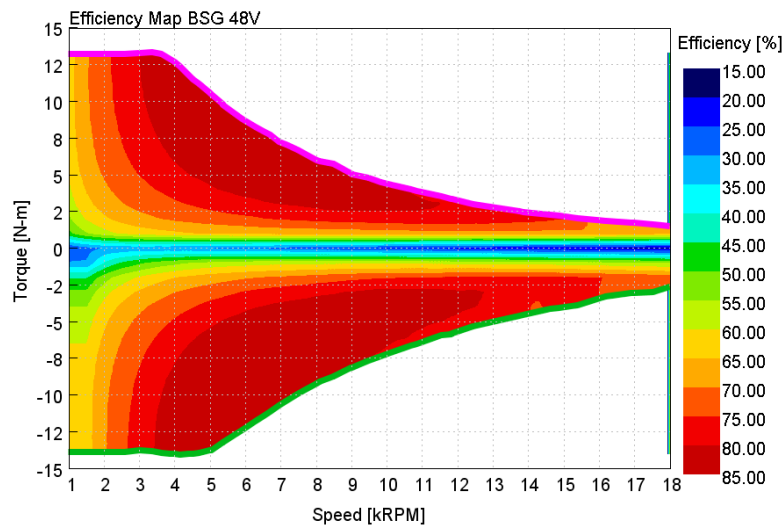


Figure 5.6 - Electric Machine efficiency map and maximum (pink) and minimum (green) torque curves [27]

As far as the energy management strategy is concerned, it is implemented in Matlab-Simulink environment and features an online power-split optimization between the internal combustion engine and the electric motor satisfying at the meantime the driver power demand defined by the driver controller. In a conventional powertrain simulation, the driver power demand required to reproduce a specified target speed or a tip-in maneuvers, is converted at each time into brake actuation and accelerator actuation. These signals, in addition to the gear number and the clutch position, defined by the requirement of using a fixed gear strategy, are used directly in the engine, transmission and clutch objects of the

model. For the electrified powertrain analysis, instead, brake/accelerator actuation, driver power demand, engine and transmission status, engine and electric motor speeds, state of charge of the battery and so on, are input for the energy management strategy.

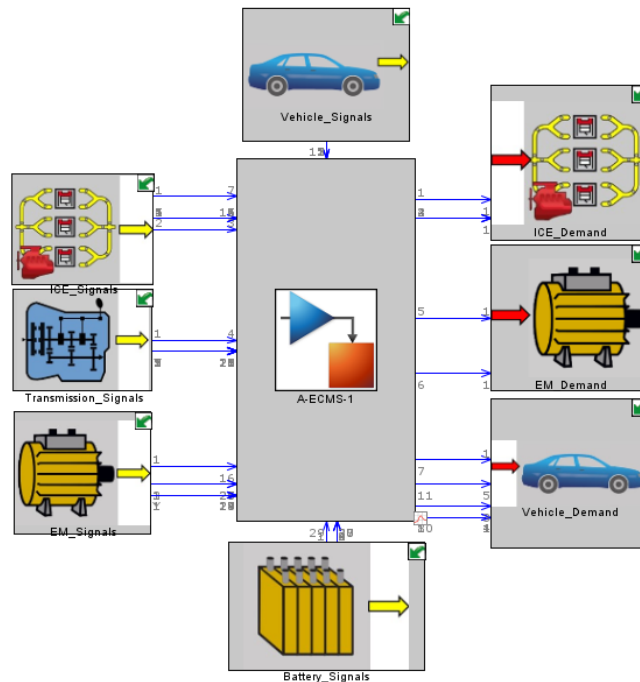


Figure 5.7 - GT-SUITE scheme of EMS [27]

5.3 Hybrid Control Modeling

The hybrid control strategy was implemented in Matlab-Simulink environment since the Simulink based controller has a higher level of flexibility than an equivalent controller implemented in GT-SUITE.

While in a conventional vehicle the internal combustion engine has to satisfy the total driver power demand, in a hybrid electric vehicle, since there are more power sources available, it is necessary to introduce an energy management system, which decides the power-split between the internal combustion engine and the electric motors. Therefore, a high-level controller, composed of two parts, must be added: the supervisory controller receives and processes information coming from the driver and the vehicle (vehicle speed, engine speed, ICE status, state of charge of the battery,...) and decides the best operation mode and the energy management system, which splits the power demand between the actuators for a given time instant.

The hybrid functionalities that can be defined by the supervisory controller for the test case vehicle are:

- Stop-Start: for vehicle speeds close to zero, the ICE is switched off to reduce the engine idling time during vehicle stops.

5 Dynamic Approach

- **Regenerative Braking:** during the deceleration phases, the kinetic energy that would be converted into thermal energy through frictional braking, is partially recovered by the electric machine and stored in battery. The regenerative braking strategy adopted consists in recover a percentage of the maximum BSG mechanical power depending on the brake pedal.

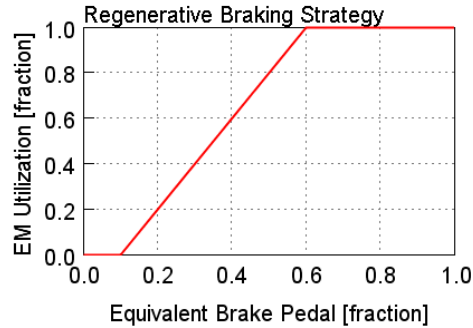


Figure 5.8 - Regenerative Braking Strategy defined through an equivalent brake pedal function [27]

- **Parallel Mode:** during the traction phase, the energy management strategy performs a power-split optimization defining the ICE and EM power demand. The energy management system implemented allows to accomplish two parallel modes: the Torque Assist consists of a reduction in the power required to the ICE and the use of the EM as a motor to compensate for the driver power demand; the Load Point Moving increases the engine load and by using the EM as a generator, the excess energy is stored in the battery.

The Electric Driving mode was excluded a priori, due to the low power of the EM of the P0 architecture investigated compared to the driver power demand during driving cycle.

The scope of the energy management strategy in this application is to minimize the fuel consumption and the Equivalent Consumption Minimization Strategy was adopted for this purpose. Once a driver power demand has been defined, different combinations of power splits can satisfy it and each of them corresponds to a different equivalent fuel consumption, as defined in 2.1 equation. The task of the EMCS is to provide the optimum power-split at each time step by minimizing the instantaneous equivalent fuel flow rate.

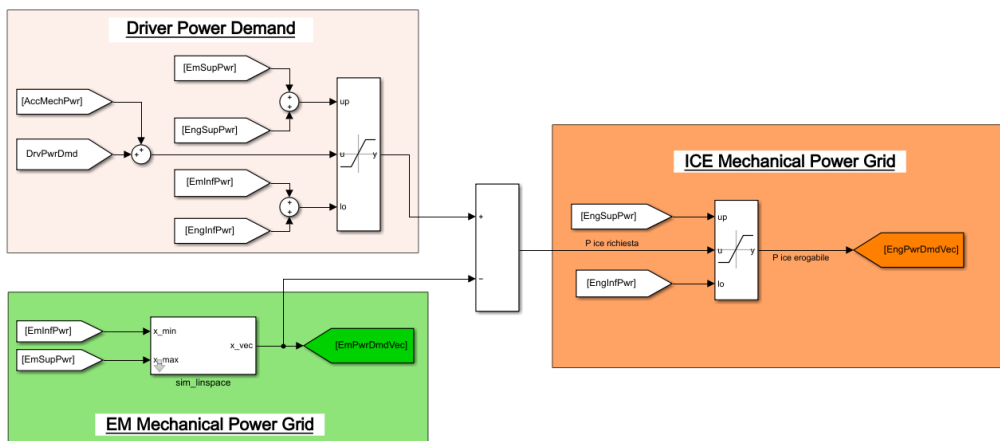


Figure 5.9 - EMS Modeling: Definition of possible power-split combination

5.3 Hybrid Control Modeling

Based on this reason, each driver power demand value defined during the vehicle simulation in GT-SUITE become an input for the Simulink model that define a set of possible power split combination. The driver power demand, such as the ICE and EM power demand, complies with the mechanical limit of the component. The model contains the full load ICE curve, the maximum and minimum torque curves of the EM and the voltage and current limitations in order to limit the relative power requested to the ICE and EM if necessary. For the evaluation of the instantaneous fuel consumption an engine fuel map is used, defined through the steady-state analysis. For the evaluation of the virtual fuel consumption, the Battery Power is calculated with a static approach depending on the electric EM power demand and on the state of charge of the battery. Regarding the equivalence factor, for this work, it was set constant and calibrated separately for each driving cycle in order to guarantee the charge sustaining condition of the battery.

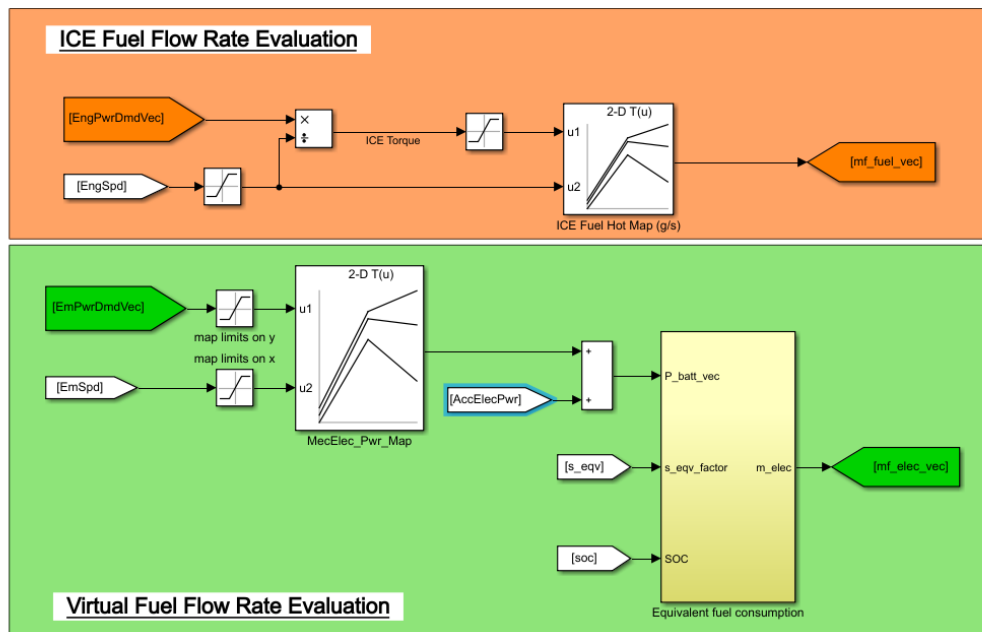


Figure 5.10 - EMS Modeling: ICE Fuel Flow Rate and Virtual Fuel Flow Rate

Finally, having obtained the values of the equivalent fuel consumption associated with each possible combination of power-split, the optimization algorithm will choose the minimum value from these, which will define the optimal power-split. In the model developed there is already implemented, but not used for this study, the possibility to take into account several penalty factors, for example a penalty could be introduced in the case in which the actual power of the engine is very different compared to the ICE power demand.

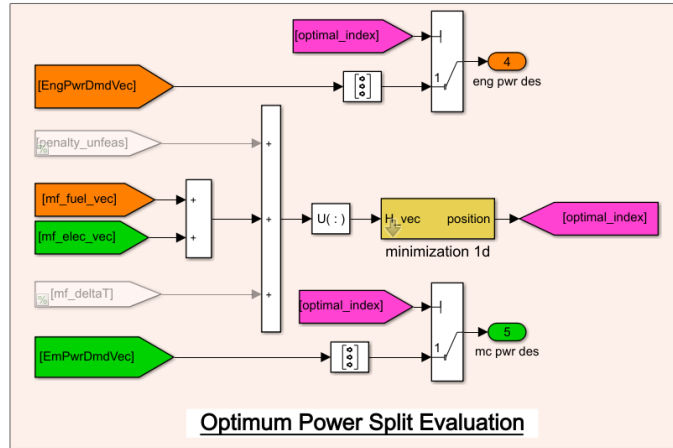


Figure 5.11 - EMS Modeling: Optimum Power Split Definition

5.4 Electric Supercharger Control Strategy

Part of the study was focused on assessing the potentialities of the eSupercharger, not only to improve performance in terms of vehicle acceleration, but also for fuel consumption reduction. Two different eSC control strategy were implemented: a rule-based control developed in GT-SUITE environment; a control strategy integrated into the EMS implemented with Matlab-Simulink routine.

5.4.1 Rule Based Control

A rule-base control for the eSupercharger was implemented in GT-SUITE that defines the eSC activation and regulation based on a threshold of difference between target and actual boost pressure. In this case, the control strategy of the eSC is not affected by the optimization operation performed by the energy management system, since the ECMS is not able to evaluate the electric power consumption during the eSC operation. Referring to the study carried out in [27], the eSC controlling strategy adopted is explained:

- The accelerator pedal, corresponding to a given driver power demand, is converted through the engine controllers and the engine performance map defined in steady-state conditions in a target boost pressure.

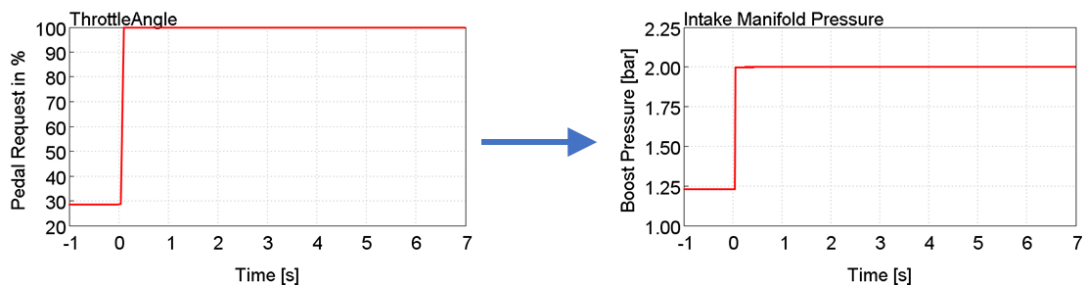


Figure 5.12 - eSC Activation Strategy - 1 [27]

5.4 Electric Supercharger Control Strategy

- In a conventional turbocharged vehicle (not electrically supercharged), due to mechanical and fluid-dynamic delays, the turbo lag phenomenon occurs: a certain amount of time is required before the actual pressure reaches the target one. During this transient, a certain ratio gap can be identified that will be the target pressure ratio for the eSupercharger.

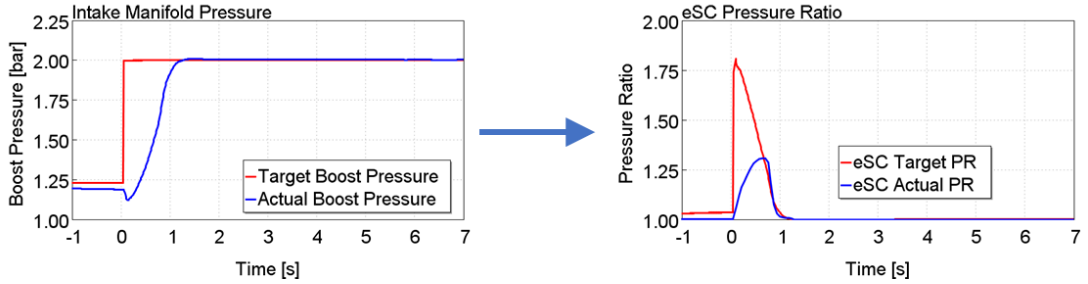


Figure 5.13 - eSC Activation Strategy - 2 [27]

- Given the eSC pressure ratio target and the corrected mass flow rate through the compressor, the eSC speed target is defined. A PI controller converts the error between the actual and the target eSC speed into an electric power demand to the motor driving the eSC.

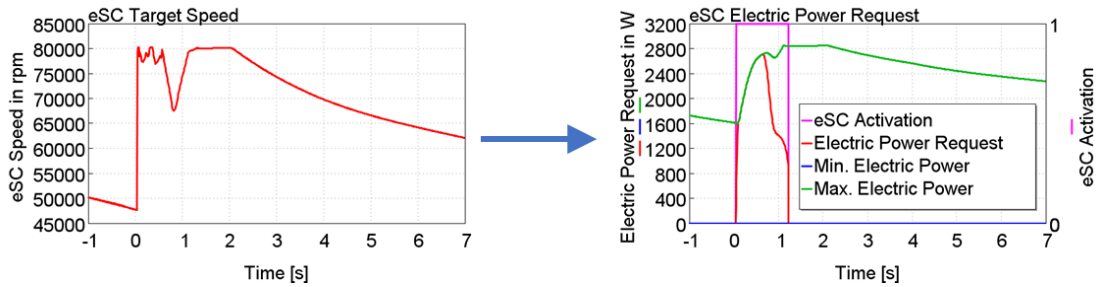


Figure 5.14 - eSC Activation Strategy - 3 [27]

The Figure 5.15 shows the flowchart of the operations performed by the eSC control strategy adopted.

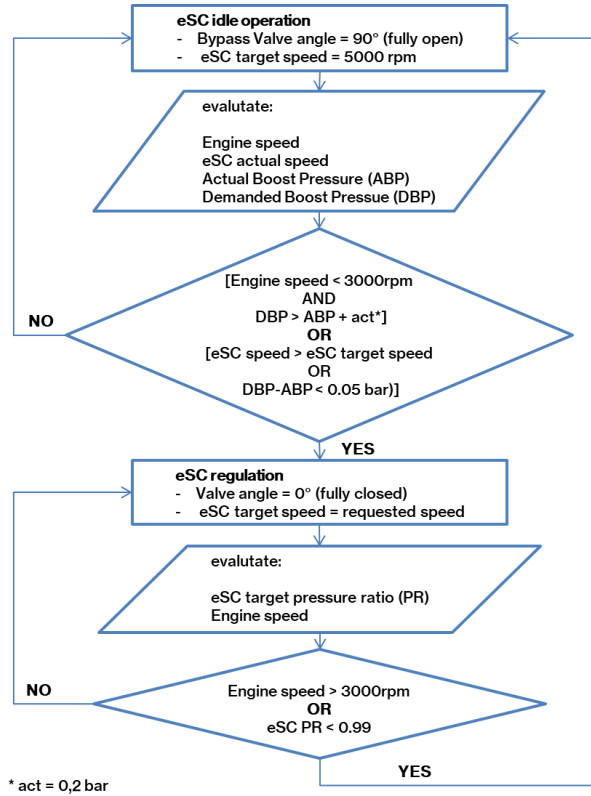


Figure 5.15 - Flowchart of the eSC rule-based control strategy

5.4.2 EMS Integrated eSC Control

The base energy management strategy handled the electric power for the ancillaries in a passive way; it was unable to provide actuation/deactivation of additional devices. To take into account the overall electric power needed by the vehicle in the powersplit operation, the base hybrid control strategy implemented has been redefined.

The eSC rule-based control strategy was integrated in the Matlab-Simulink routine that define the optimum powersplit through the ECMS technique. For each powersplit combination, an eSC electric power consumption is evaluated and converted in equivalent fuel flow rate. The additional energy requirement is considered in the minimization of the instantaneous equivalent fuel flow rate. The electric power related to the eSC utilization is computed as the sum of the required electric power, defined in steady-state condition, and a transient contribution related to the inertia power during eSC acceleration. This contribute is evaluated with a simplified formula reported in Equation 3.1:

$$P_{in} = k (eSC_{TgtSpd} - eSC_{ActSpd}) \cdot eSC_{ActSpd} \quad (3.1)$$

Where eSC_{TgtSpd} is the eSC speed demand, eSC_{ActSpd} is the actual speed and k is a tuning parameter optimized to have a good agreement between the P_{in} value predicted by the ECMS and the P_{in} evaluated in GT-SUITE. In this way, the ECMS is able to consider the overall electric power related to each possible powersplit combination.

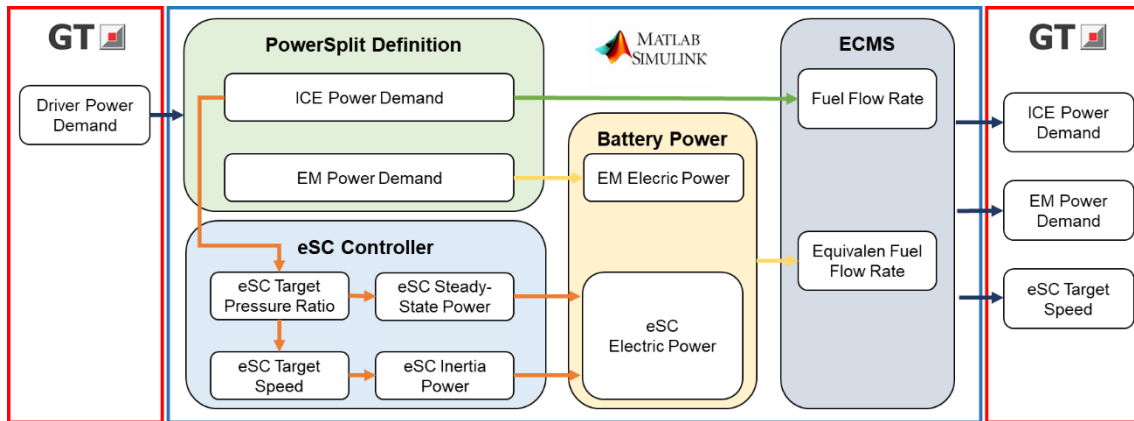


Figure 5.16 - Schematic representation of the update Hybrid Control Strategy for the eSC Control and Powersplit Optimization

5.5 Case study

The study carried out aims to evaluate five different powertrain configurations: a conventional powertrain concept equipped with a stoichiometric turbocharged gasoline engine (B-SUV(1)); four different 48V electrified powertrain concepts, the first featuring a Belt Starter Generator mild-hybrid architecture (B-SUV(2)), the second featuring in addition to the BSG an high efficiency engine (B-SUV(3)) and the others featuring, in addition to the previous mentioned solutions, an engine Millerization combined with an e-supercharger controlled in one case by a rule based strategy (BSUV(4)) not implemented in the hybrid control strategy, and in the other by integrating the contribute of the eSC power consumption in the optimization operation provided by the ECMS (BSUV(4-a)).

Legend	Engine	Hybrid Architecture	eSC	EMS
B-SUV(1) ■	Ref. Engine	X	X	X
B-SUV(2) ■	Ref. Engine	P0 48V	X	ECMS
B-SUV(3) ■	Engine A	P0 48V	X	ECMS
B-SUV(4) ■	Engine C	P0 48V	✓	ECMS
B-SUV(4-a) ■	Engine C	P0 48V	✓	ECMS-update

Legend	CR	eSupercharger	Valve Strategy
Reference Engine	9.8	X	MultiAir
Engine A	12	X	MultiAir
Engine C	12	✓	MultiAir & Miller

All the powertrain configurations investigated were equipped with the same 6-speed manual transmission, whose technical specifications are reported in Table 4.3.

As far as the conventional powertrain concept (B-SUV(1)) is concerned, it features the same characteristics of the vehicle investigated in Chapter 4, which are reported in Table 4.2.

5 Dynamic Approach

Regarding the electrified vehicles concepts, the vehicle test mass was increased by 20 kg representing the additional weight of the BSG and the battery employed in the dual voltage electric network. The main technical data of the electric devices adopted are reported in Table 5.2.

Parameter	Unit	NEDC	WLTC	RTS-95
Electrified Vehicle Test Mass	kg	1470	1630	1630
Rolling Radius	m	0.333	0.333	0.333
Drag. Coeff. X Frontal Area	-	0.82	0.93	0.93
Electrical Load	[W]	220	400	400

Table 5.1 - Electrified Vehicle Main Specifications for NEDC, WLTC and RTS_95

	Parameter	12 V	12 + 48 V
Alternator	Peak Power Motor	0 kW	5.5 kW
	Peak Power Generator	3.4 kW	7.5 kW
Starter	Peak Mechanical Power	1 kW	1 kW
Battery	Capacity (12 V)	60 Ah	60 Ah
	Capacity (48 V)	NA	10 Ah

Table 5.2 - Electric Devices Technical Data

For fuel consumption evaluation, three driving cycles were selected: the New European Driving Cycle (NEDC), the Worldwide Harmonized Light-Duty Test Cycle (WLTC) and a more dynamic RDE driving cycle, the RTS-95. The gear shift is imposed on NEDC according to UNECE 83 [30] while on WLTC and RTS-95, according to [6], the gear shift pattern was computed by means of the Heinz Steven tool available in [31].

Regarding the assessment of the performance on the driving cycles, it should be pointed out that all results obtained are computed assuming null added or depleted energy in battery system. To do so, the correction proposed in [6] for HEV was used. This standard requires that a HEV should undergo several tests in order to have a statistically valid correlation between the fuel consumption and the added or depleted energy in the entire battery storage system. In this way it is possible to define a correlation between fuel consumption and energy in the battery so that the fuel consumption at balanced energy in the battery can be computed. This method involves running the vehicle model simulation twice on the same driving cycle with different starting battery state of charge. The final fuel consumption value is then computed making the weighted average of the fuel used on the electric energy drained or added to the battery over the two tests [36].

In addition to fuel consumption assessment, the attention was also focused on vehicle transient performance evaluated on five typical maneuvers:

- 0 – 100 km/h
- 60 – 100 km/h in V gear
- 80 – 120 km/h in VI gear
- 40 – 80 km/h in IV gear
- 60 – 80 km/h in VI gear

In order to have a comparison parameter of the improvements in terms of performance, a Performance Index (PI) was introduced, as defined in Equation 5.1.

$$PI = \frac{3600}{v_{max}} + t_{0-100} + t_{60-100} + t_{80-120} \quad (5.1)$$

where the three terms are the performance time for the 0 – 100 km/h acceleration and for the 80 – 120 km/h and 60 – 80 km/h elasticity maneuvers in VI gear.

5.6 Results

This section presents the results of the electrified powertrain configurations comparing with those of the conventional vehicle. The focus is on the potential of 48V electrification; the adoption of Miller cycle for a stoichiometric turbocharged gasoline engine; the energy management strategy capabilities to manage the electric boosting. The effectiveness of the engine technologies adopted and the eSC control strategies developed was evaluated both in terms of fuel consumption and vehicle performance.

5.6.1 Fuel Consumption Evaluation

In this section the fuel consumption of the investigated powertrain concepts is reported and discussed. The Figure 5.17 shows the normalized CO₂ emissions values.

Legend	Engine	Hybrid Architecture	eSC	EMS
B-SUV(1)	Ref. Engine	X	X	X
B-SUV(2)	Ref. Engine	P0 48V	X	ECMS
B-SUV(3)	Engine A	P0 48V	X	ECMS
B-SUV(4)	Engine C	P0 48V	✓	ECMS
B-SUV(4-a)	Engine C	P0 48V	✓	ECMS-update

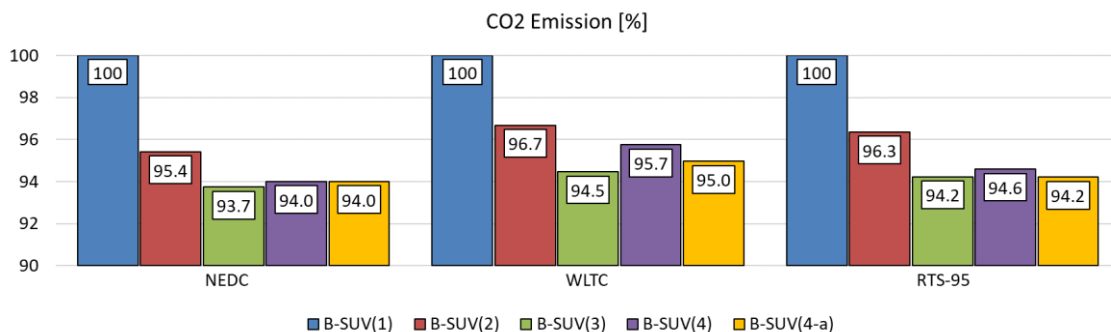


Figure 5.17 - Normalized CO₂ Emissions for the NEDC, WLTC and RTS-96 driving cycles

The electrified vehicle configuration BSUV(2) provides a benefit in terms of fuel consumption reduction of around 4.6% on NEDC and of 3.3% and 3.7% on WLTC and RTS-95 respectively compared to the conventional powertrain concept BSUV(1). The electrified vehicle concept can

5 Dynamic Approach

exploit the power available on board in the battery: during the deceleration phases it is possible to store energy in the battery and then use it for traction purposes.

An additional fuel consumption improvement of 1.7% on the NEDC and of about 2% on WLTC and RTS-95 can be noticed with the adoption of the high efficiency Engine A (BSUV(3)).

Regarding the electrified vehicle configuration featuring the combined adoption of Millerization and electric boosting (BSUV(4)) with respect to the base powertrain configuration, a 6% reduction of CO₂ emissions is achieved on NEDC and 4.3% and 5.4% on WLTC and RTS-95 respectively.

As far as the eSC control strategy is concerned, a further improvement of about 0.8% and 0.4% on WLTC and RTS-95 is obtained. On the NEDC the integration of the eSC control strategy in the ECMS does not bring any benefits as the power required to perform the driving cycle does not require the electric supercharging.

In Figures 5.18 and 5.19 is reported a deeper investigation regarding the effectiveness of the power split operation on the NEDC for the electrified powertrain B-SUV(2) concept.

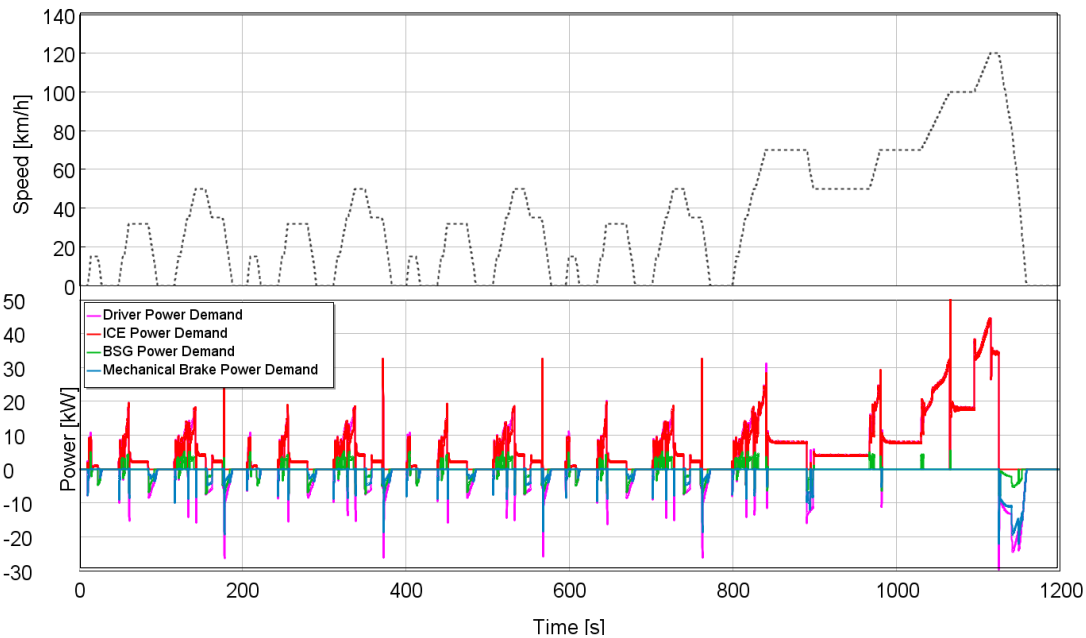


Figure 5.18 - EMS Power Split for NEDC driving cycle for B-SUV(2) configuration

Figure 5.18 shows the optimum power split between the internal combustion engine and the electric machine performed by the Equivalent Consumption Minimization Strategy for the NEDC. During the deceleration phases of the driving cycle, the BSG power demand is negative: the BSG is used in generator mode storing the electric energy into the battery. In the traction phases, the BSG power demand is positive especially during the lunch phases, in which, according to the energy management system, is convenient to decrease the engine load. It can be noticed that the load point moving point is never actuated on NEDC cycle, since the availability of electric energy recovered with regenerative braking is sufficient for the traction phases satisfying the charge sustaining condition. The same consideration was also found on the RTS-95 and NEDC driving cycles. In Figure 5.29 is reported a reduced time frame of the NEDC: in the bottom part the benefit of the power split is highlighted, comparing both the instantaneous and the cumulated fuel consumption of the conventional and electrified powertrain concepts, B-SUV(1) and B-SUV(2) respectively.

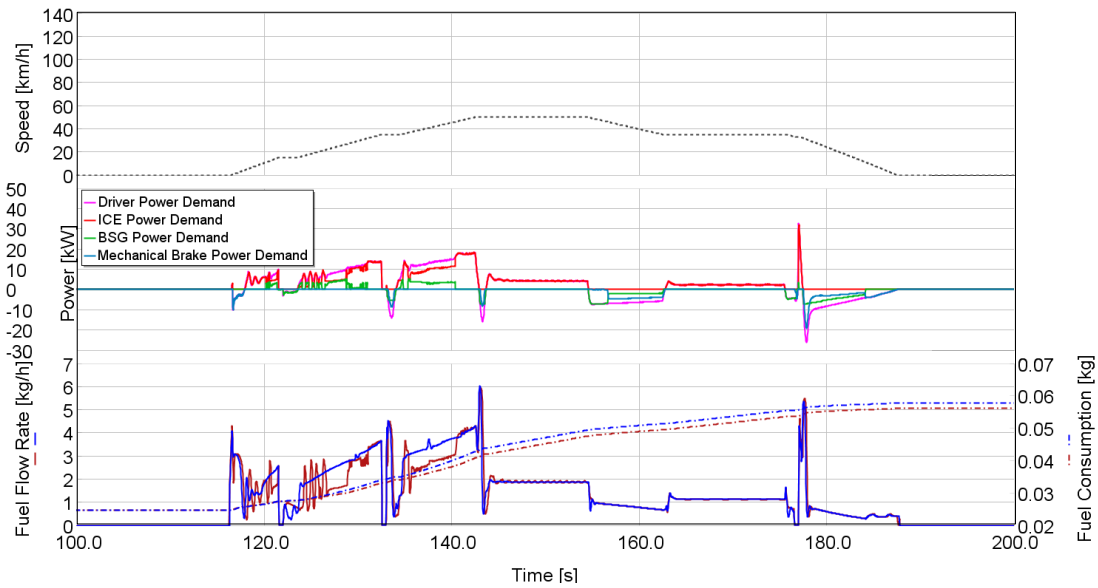


Figure 5.19 - Fuel Consumption Comparison between B-SUV(1) and B-SUV(2) and EMS Power Split for B-SUV(2) on 100 – 200 s time frame of the NEDC

In Figure 5.20 is reported the energy used by the eSC operation and the BSG operation for propulsion on the RTS-driving cycles. The adoption of the eSupercharger leads to a reduction of the electric machine operation, as it can be seen comparing the red and the green lines related to B-SUV(2) and B-SUV(3) with the BSG energy consumption line of the B-SUV(4). These difference are due to the electric boosting operation that cannot be controlled by the energy management system resulting in a real electrical load, therefore, in order to ensure the charge sustaining condition, a reduction of the electric machine energy consumption must be obtained.

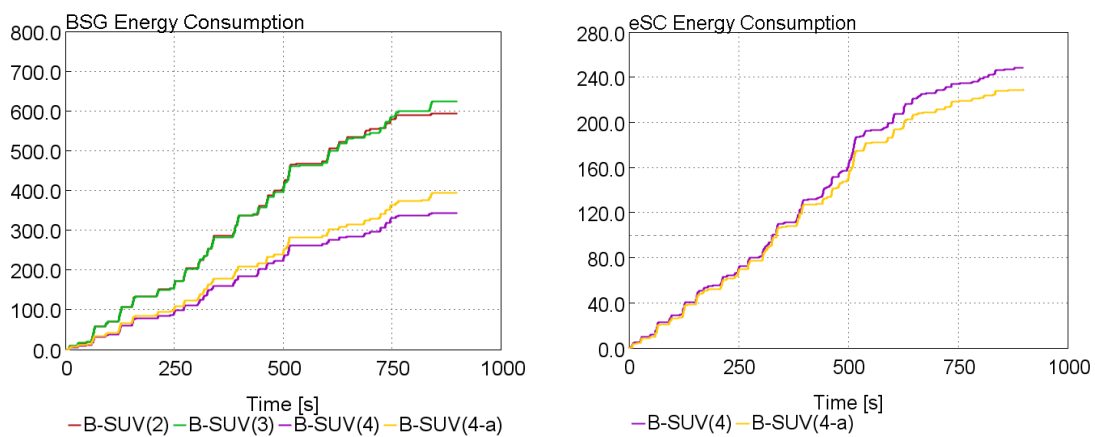


Figure 5.20 - Energy BSG and Energy eSC Consumption comparison for RTS-95 driving cycle.

The update ECMS-I, that takes into account the energy consumption resulting from an eSC operation, reduces the ICE load, reducing consequently the eSC activation, and increases the power demand to the electric machine. The update ECMS is quite effective on the WLTC (-1.4 g/km CO₂) and the RTS-95 cycle (-0.9 g/km CO₂). On the NEDC, where the eSC operation is not required, it provides the same results of the previous ECMS.

5.6.2 Transient Maneuvers Analysis

In Figure 5.21 the results concerning the elasticity maneuvers are reported.

Legend	Engine	Hybrid Architecture	eSC	EMS
B-SUV(1) ■	Ref. Engine	X	X	X
B-SUV(2) ■	Ref. Engine	P0 48V	X	ECMS
B-SUV(3) ■	Engine A	P0 48V	X	ECMS
B-SUV(4) ■	Engine C	P0 48V	✓	ECMS
B-SUV(4-a) ■	Engine C	P0 48V	✓	ECMS-update

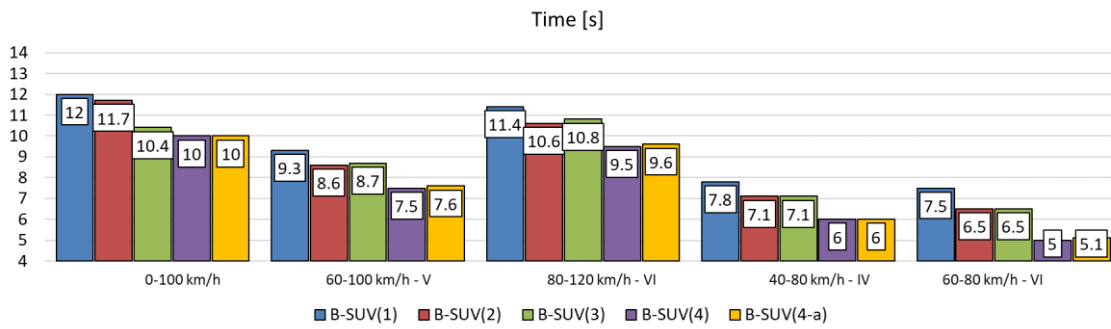


Figure 5.21 - Transient Maneuvers Performance Time

Considering the acceleration from 0 to 100 km/h, an improvement of 0.7 s of performance time is achieved with the BSG Torque-Assist (B-SUV(2)) compared to the conventional powertrain configuration. A further reduction of 1.3 s is obtained with the adoption of the Engine A concept (high efficiency engine) in the electrified powertrain. The combined effect of the Millerization cycle and the e-boosting featuring by the B-SUV(4) allows to achieve a reduction of 2 s with respect to the conventional vehicle concept.

As far as the elasticity manoeuvres are concerned, the electrified B-SUV(2) and B-SUV(3) vehicles concept are able to reduce the time required for the manoeuvres by around 0.7 s on the 60 to 100 km/h in V gear, on 80 to 120 km/h acceleration and on 40 to 80 km/h in IV gear and improve the performance time by 1 s on the 60 to 80 km/h acceleration. The integration of the electric supercharger (B-SUV(4) and B-SUV(4-a)) improves the transient response of the engine, lowering the elasticity time of 1 s on average compared the others electrified powertrain concepts and reaching 2 s of global reduction with respect to the conventional powertrain configuration. These two electrified powertrain concepts take advantage from the battery power availability that allows the simultaneous operation of the BSG and the eSC. The implementation of the eSC control strategy in the hybrid control strategy, used in the B-SUV(4-a) concept, does not lead to considerable difference in terms of transient response compared to the B-SUV(4) featuring the rule-based eSC control. During tip-in operation the full load performance of the engine is required, consequently the activation of the eSC operation depends only on the rule-based strategy that is not modified for the two vehicles concepts.

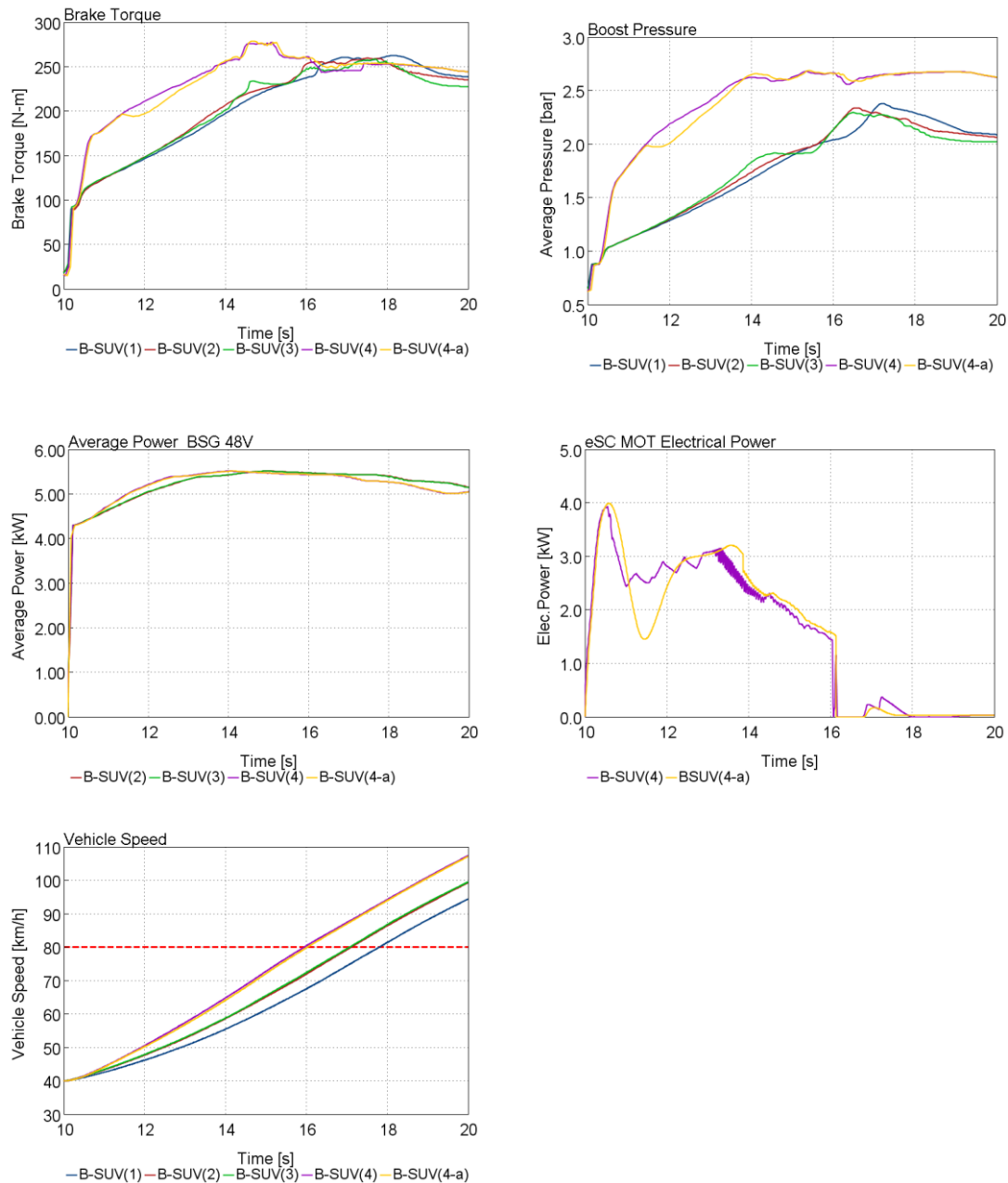


Figure 5.22 - Detail of the 40 – 80 km/h in IV gear manoeuvre

Figure 5.22 shows a deeper investigation in the first 10 s of the 40 – 80 km/h in IV gear manoeuvre. It is possible to note that the electrified vehicle concepts B-SUV(2) and B-SUV(3) achieved an improvement in performance time compared to the conventional vehicle concept, despite the ICE brake torques raise almost identically; the Torque Assist functionality exploited by the 48V BSG increases the shaft power. Regarding the B.SUV(4) and B-SUV(4-a), the integration of the eSC remarkably enhances the transient response of the engine; thanks to the electric boosting the boost pressure increases very rapidly filling the lack of response shows by the traditional turbocharged engines.

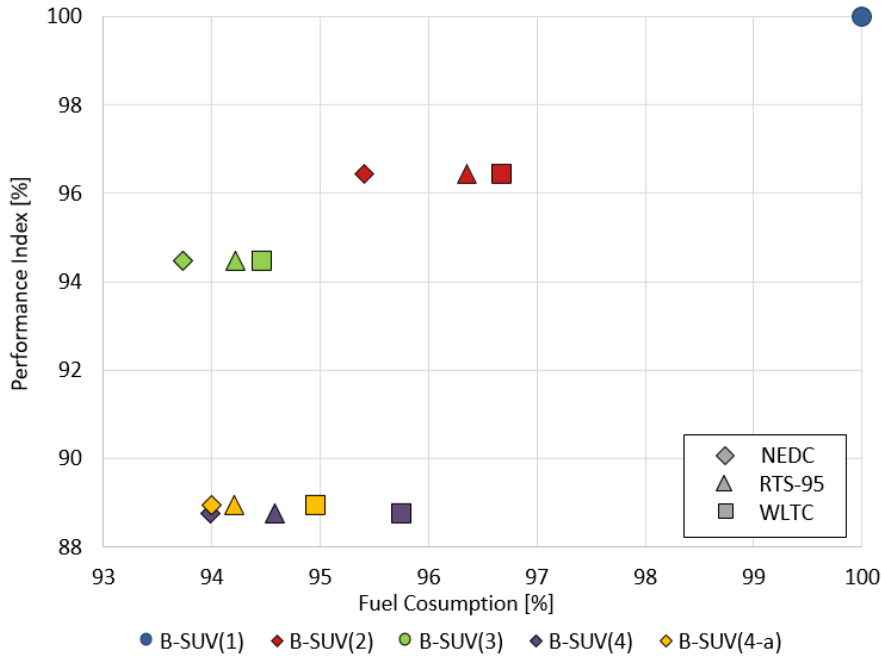


Figure 5.23 – Normalized Performance Index vs Normalized Fuel Consumption evaluated on NEDC, WLTC and RTS-95

In order to compare in a synthetic way the results in terms of transient performance and fuel consumption, the Performance Index, according to Equation (5.1) was computed for all the powertrain configurations investigated. In figure 5.23, a performance summary in terms of normalized performance index vs. normalized fuel consumption on NEDC, WLTC, RTS-95 is reported. The 48V electrification of the powertrain enhances significantly the vehicle performance (PI reduction up to 3.5% compared to the conventional powertrain), while the fuel economy benefits are around 4.6% on NEDC, 3.3% on WLTC and 3.7% on RTS-95 compared to the conventional vehicle configuration. The adoption of a high efficiency engine combined with the electrification (B-SUV(3)) provides an additional improvement of the vehicle performance reducing the PI of about 2.2% with respect to the electrified powertrain B-SUV(2) and achieved the highest benefits in terms of CO₂ emissions reduction on all the driving cycles investigated: - 6.3% on NEDC, -5,5 on WLTC and 5.8 on RTS-95 compared to the base powertrain concept. For the B-SUV(4), whose engine features an increased CR and exploited the potentiality of the e-boosting and a Miller Cycle, is able to dramatically reduce the turbo lag phenomenon due to the instantaneous supercharging response provided by the electric supercharger. The result is an further improvement of the PI of about 6% with respect to the electrified concept B-SUV(3) achieving an impressive 11% of performance enhancing compared to the conventional powertrain vehicle; moreover, B-SUV(4) concept is able to reduce the fuel consumption of about 6% on NEDC and 4.3% and 5.4% on WLTC and RTS-95 respectively. Finally, B-SUV(4-a) does not lead to considerable difference in terms of PI compared to the B-SUV(4), since independently from the eSC energy management, during elasticity manoeuvres the full load performance of the engine is required and the activation of the eSC depends only on the rule based strategy. On the other hand, the optimal powersplit provided by the update ECMS, that takes into account the eSC energy consumption, leads to a further improvement of 0.7% on the WLTC (-1.4 g/km CO₂) and the 0.4% RTS-95 cycle (-0.9 g/km CO₂) compared to B-SUV(4).

6 Conclusions

An innovative hybrid control strategy for mild-hybrid 48V powertrains has been developed and its effectiveness has been tested among different driving cycles. This energy management strategy takes into account the overall electric energy of engine ancillaries not devoted directly to traction. In this study an electrical supercharger has been chosen as electrical ancillaries to be included in the system and to be investigated. It represents a possible electrical device that the increased electrification level of the vehicles allows to integrate achieving important improvement in vehicle performance.

As far as steady-state analysis is concerned, different engine concepts were investigated to assess the potential of the increase in the compression ratio and the adoption of Miller cycle for a stoichiometric turbocharged gasoline engine. At partial load the higher compression ratio leads to a benefit of 3% on average in terms of engine efficiency. At full load taking advantage of the Miller cycle is obtained a significant increase in the maximum brake torque in the low speed region (more than 40% at 1250 RPM).

The reduction of CO₂ emissions achievable with the electrified powertrain is around 4% and an additional 1.5% of benefits has been obtained with the adoption of the eSupercharger, the Miller cycle and the CR 12. At this point the base ECMS was updated including the electric power of the eSC. This electric power is composed by a steady-state eSC power demand and a transient power due to the inertia contribution needed to activate the eSC. For the NEDC the update of the ECMS does not lead to benefits in terms of fuel consumption; on the other hand, it leads to a further improvement of 0.7% on the WLTC (-1.4 g/km CO₂) and 0.4% RTS-95 cycle (-0.9 g/km CO₂).

An innovative energy management strategy that takes into account also the electrical ancillaries has been developed. The results are promising for what concern low cycles and aggressive cycles. This EMS can be validated on different case study, as for example the adoption of the eSC upstream of the TurboCharger. Additional ancillaries can be included in the system like for example an eCatalyst and to extend the assessment of the EMS also for a cold-start driving cycle.

Bibliography

- [1] Kumawat, A., Thakur, A., “A comprehensive Study of Automotive 48-Volt Technology”, SSRG International Journal of Mechanical Engineering, Volume 4(5), Pages 7-14, May 2017, doi:[10.14445/23488360/IJME-V4I5P103](https://doi.org/10.14445/23488360/IJME-V4I5P103).
- [2] Lutsey, N., “Transition to A Global Zero Emission Vehicle Fleet: A Collaborative Agenda for Governments”, ICCT White Paper, 2015.
- [3] Transportation Research Board and National Research Council. “Overcoming Barriers to Electric-Vehicle Deployment: Interim Report” Washington, DC: The National Academies Press, 2013 doi:10.17226/18320.
- [4] Corporate Magazine FEV, <http://magazine.fev.com/en/fev-study-examines-drivetrain-topologies-in-2030-2>, accessed on July 2019.
- [5] Onori, S., Serrao, L., Rizzoni, G., “Hybrid Electric Vehicles Energy Management Strategies”, ISBN 978-1-4471-6781-5, 2016, doi:10.1007/978-1-4471-6781-5.
- [6] [COMMISSION REGULATION \(EU\) 2017/1151, Official Journal of European Union, L 175, 7/7/2017, p. 1-643.](#)
- [7] Scharf, J., Thewes, M., Balazs, A., Fh, D., Lückenbach, S., Speckens, F., “All Clean Gasoline Hybrid Powertrains – Real Driving Emissions, Lambda = 1 & Euro 7”, Proceedings of the 27th Aachen Colloquium Automobile and Engine Technology, 2018, pp. 935–956, Aachen, Germany, October 8-10, 2018.
- [8] Chomat, M., “New Applications of Electric Drives”, ISBN:978-953-51-2233-3, 2015, doi:10.5772/60584.
- [9] The International Council on Clean Transportation, <https://theicct.org/sites/default/files/Global-Fuel-Economy-Policies-Overview-ICCT-ZYang-20032018.pdf>, accessed on July 2019.
- [10] Rolando, L., “An innovative methodology for the development of HEVs energy management systems”, PhD Thesis, Politecnico di Torino (Torino, Italy), 2012.
- [11] Ehsani, M., Gao, Y., Gay, S., Emadi, A., “Modern electric, hybrid electric, and fuel cell vehicles: fundamentals, theory, and design”, ISBN:978-142-00-5400-2, 2009.

-
- [12] X-Engineer, Mild Hybrid Electric Vehicle, <https://x-engineer.org/automotive-engineering/vehicle/hybrid/mild-hybrid-electric-vehicle-mhev-architectures/>, accessed on July 2019.
- [13] X-Engineer, Mild Full Hybrid Electric Vehicle, <https://x-engineer.org/automotive-engineering/vehicle/hybrid/micro-mild-full-hybrid-electric-vehicle/>, accessed on July 2019.
- [14] E. Erich; ADD Solution; “Voltage Classes & 48 Volt Application For Mild Hybrid Vehicles And High Power Loads”; February 2017, BIS Group, Automotive 48 Volt Power Supply and Electrification Systems.
- [15] X-Engineer, Mild Hybrid Electric Vehicle, <https://x-engineer.org/automotive-engineering/vehicle/hybrid/mild-hybrid-electric-vehicle-mhev-introduction/> (accessed on July 2019)
- [16] AVL UK Expo 2014 / Ulf Stenzel, “48V Mild Hybrid Systems Market Needs and Technical Solutions”, AVL Engineering and Technology, https://gansystems.com/wp-content/uploads/2016/07/AVL_UK_Expo_48V_Mild_Hybrid_Systems.pdf
- [17] Aymanns, R., Uhlmann, T., Nebbia, C., Plum, T., “Electric Supercharging new opportunities with higher system voltage”, MTZ Worldw, Volume 75(4), 2014, doi:10.1007/s38313-014-0166-0
- [18] Borg Warner, Electric Boosting, <https://www.borgwarner.com/technologies/electric-boosting-technologies>, accessed on July 2019.
- [19] M. Chomat, “New Applications of Electric Drives”, AvE4EvA Publ., 2015.
- [20] Bertsekas, D., “Dynamic Programming and Optimal Control”, ISBN:978-188-65-2908-3, 2005.
- [21] Geering, H.P., “Optimal Control with Engineering Applications”, ISBN: 978-3-540-69438-0, 2007, doi: 10.1007/978-3-540-69438-0.
- [22] Barbero, L., “Ottimizzazione della strategia di controllo e valutazione delle potenzialità di un sistema di propulsione ibrido a 48 volt per autovetture”, Master Thesis, Politecnico di Torino (Torino, Italy), 2017.
- [23] Musardo, C., Rizzoni, G., Guezennec, Y., Staccia, B., “A-ECMS: An adaptive algorithm for hybrid electric vehicles energy management”, European Journal Of Control, Volume 11, Issues 4–5, Pages 509-524, 2005, doi:10.3166/ejc.11.509-524.
- [24] Gamma Technologies, GT-POWER Engine Simulation Software, “Engine Performance Analysis Modeling,” GT-Suite.
- [25] Gamma Technologies, GT-SUITE example of SI engine model.
-

0 Bibliography

- [26] Ruggiero, A., Montalto, I., Poletto, P., Pautasso, E., Mustfaj, K., Servetto, E., "Development and assessment of a Fully-physical 0D Fast Running Model of an E6 passenger car Diesel engine for ECU testing on a Hardware-in-the-loop system", Proceedings of the International Congress SIA Powertrain – Rouen, France, May 21-22, 2014.
- [27] Accurso F. "Development through numerical simulation of an innovative energy management strategy for a 48V Mild-Hybrid vehicle", Master Thesis, Politecnico di Torino (Torino, Italy), 2018.
- [28] Luisi, S., Doria, V., Stroppiana, A., Millo, F. et al., "Experimental Investigation on Early and Late Intake Valve Closures for Knock Mitigation through Miller Cycle in a Downsized Turbocharged Engine," SAE Technical Paper 2015-01-0760, 2015, <https://doi.org/10.4271/2015-01-0760>.
- [29] Guzzella, L., Sciarretta, A., "Vehicle Propulsion Systems: Introduction to Modeling and Optimization" ISBN:978-3-642-35913-2, 2007, doi: 10.1007/978-3-642-35913-2.
- [30] DIRECTIVE 2007/46/EC, Official Journal of European Union, L 263, 9/10/2007, p. 1–160.
- [31] UNECE Wiki, Gearshift calculation tool, <https://wiki.unece.org/display/trans/Gearshift+calculation+tool>, accessed July 2019.
- [32] Diesel Net, Emissions Test Cycles, <https://www.dieselnets.com/standards/cycles/index.php#eu-ld>, accessed on July 2019.
- [33] Corporate Magazine FEV, <http://magazine.fev.com/en/fev-hecs-ecobrid-with-48v-hybridization/>, accessed on July 2019.
- [34] Automotive Design and Production, <https://www.adandp.media/articles/continental-engineering-the-future>, accessed on July 2019.
- [35] Gamma Technologies, "GTISE Help-Vehicle Controls"
- [36] Zanelli, A., Millo, F., and Barbolini, M., "Driving Cycle and Elasticity Manoeuvre Simulation of a Small SUV Featuring an Electrically Boosted 1.0 L Gasoline Engine," SAE Technical Paper 2019-24-0070, 2019